

Boundary topological entanglement entropy in two and three dimensions

Jacob C. Bridgeman,^{1,*} Benjamin J. Brown,² and Samuel J. Elman^{2,3,4}

(Authors listed alphabetically)

¹*Perimeter Institute for Theoretical Physics, Waterloo, Ontario, Canada*

²*Centre for Engineered Quantum Systems, School of Physics,*

The University of Sydney, Sydney, NSW 2006, Australia

³*Department of Physics, Imperial College London, London, SW7 2AZ, United Kingdom*

⁴*School of Physics and Astronomy, University of Leeds, Leeds LS2 9JT, United Kingdom*

The topological entanglement entropy is used to measure long-range quantum correlations in the ground state of topological phases. Here we obtain closed form expressions for topological entropy of (2+1)- and (3+1)-dimensional loop gas models, both in the bulk and at their boundaries, in terms of the data of their input fusion categories and algebra objects. Central to the formulation of our results are generalized \mathcal{S} -matrices. We conjecture a general property of these \mathcal{S} -matrices, with proofs provided in many special cases. This includes constructive proofs for categories of ranks 2-5.

I. INTRODUCTION

The classification of topological phases is central to the study of modern condensed matter physics [1–4]. Moreover, they have properties that may be valuable for the robust storage and manipulation of quantum information [5, 6]. Their characteristics include a stable gap at zero temperature and quasiparticle excitations with non-trivial braid statistics [7, 8].

An important class of topological phases are represented by topological loop-gas models [9, 10]. These models can be defined in terms of an input unitary fusion category, and their ground states by superpositions of string diagrams labeled by objects from the category. The categorical framework provides a collection of local relations that ensure topological invariance of the ground states. In (2+1)-dimensions, these models are called Levin-Wen (LW) models [9]. LW models have point-like excitations, commonly called anyons, with non-trivial fusion rules and braid statistics. In (3+1)-dimensions, the input category must be equipped with a premodular braiding, leading to a Walker-Wang (WW) model [10]. Generically, WW models support point-like and loop-like excitations. In contrast to LW models, the excitations in the bulk of a WW model may be trivial, specifically if the input category is modular.

Loop-gas models can be defined on manifolds with boundaries by modifying the local relations governing the strings in the vicinity of the boundary. One way to define a boundary to a topological loop-gas is to allow some strings to terminate on the boundary. This is captured in the current work using particular objects called algebras [11, 12]. Despite their trivial bulk excitations, WW models may have highly non-trivial boundary excitations. In particular, the boundary excitations may be described by a LW model.

Intimately connected to the topological properties of these phases is the long-range entanglement present in the ground state of the Hamiltonians describing these phases [13, 14]. The long-range quantum correlations found in the ground states of topological phases can be measured using the topological entanglement entropy [15–17]. We typically expect that the entanglement entropy shared between two subsystems of the ground state of a gapped many body system to respect an area law [18]. However, supposing a sensible choice of bipartition, the entanglement entropy of the ground state of topological phases has a constant universal correction [15]. In (2+1)-dimensions, it is known that this correction relates to the total quantum dimension of the quasiparticle excitations supported by the phase [16, 17]. We can also evaluate the quantum dimensions of individual excitations [19] and defects [20, 21] of a phase using topological entanglement entropy. Other work has shown we can use the topological entanglement entropy to calculate the fusion rules [22] and braid statistics [23] of (2+1)-dimensional phases.

Generalizations of topological entanglement entropy diagnostics have been found [24, 25] for three-dimensional phases with bulk topological order. These diagnostics were first demonstrated using the three-dimensional toric code model [26] as an example. This phase gives rise to one species of bosonic excitation that braids non-trivially with a loop-like excitation in the bulk of the system. In contrast, particular classes of Walker-Wang models [10] have been shown to behave differently using the same diagnostics. Modular examples of these models demonstrate zero bulk

* jcbridgeman1@gmail.com; jcbridgeman.bitbucket.io; ORCID:0000-0002-5638-6681

topological entanglement entropy [27, 28], even though, at their boundary, they realize quasiparticle excitations with non-trivial braid statistics [27].

In Ref. 29, two new diagnostics were found to interrogate the long-range entanglement at the boundary of a three-dimensional topological phase. The behavior of the diagnostics was determined by making quite generic considerations of the support of creation operators for topological excitations, without assuming any knowledge of the underlying particle theory of the phase. It was shown that the diagnostics will show a null outcome only if all the particles that can be created at the boundary have trivial braid statistics. Conversely, boundary topological order must necessarily show positive topological entanglement entropy if quasi-particles that demonstrate non-trivial braid statistics can be created. In that work, the diagnostics were tested at the different boundaries of the three-dimensional toric code where negative outcomes were obtained at boundaries where the appropriate types of particles condense. However, a limitation of the diagnostics presented in that paper is that the meaning of a positive outcome is not well understood.

From the input fusion category perspective, the topological entanglement entropies can be understood as arising from constraints on the ‘string flux’ passing through a surface. In (3+1)-dimensions, there are also additional corrections due to braiding. Allowing strings to terminate in the vicinity of a physical boundary alters the flux (and braiding) constraints in the vicinity, thereby altering the topological entropy.

In this work, we obtain closed form expressions for bulk and boundary topological entanglement entropy diagnostics for topological loop-gas models. We obtain our results by evaluating the entanglement entropy of various regions of ground states of Levin-Wen and Walker-Wang models. This requires careful analysis of various string diagrams, such as generalized \mathcal{S} -matrices which encode the braiding properties of the input category. Additionally, we examine how the inclusion of boundaries, via algebra objects, alter these diagrams, and so the topological entropy. In all cases, we find that the entropy can be expressed in terms of the quantum dimension of the input category and the quantum dimension of the algebra object. In the bulk of (3+1)-dimensional models, we conjecture, and prove in many cases, that the entropy is the logarithm of the total quantum dimension of the particle content of the theory, extending the results of Ref. 28.

Overview

Following a brief summary of our results, the remainder of this paper is structured as follows. In Section II, we provide some mathematical definitions and minor results that are required for the remainder of the paper. In Section III, we briefly review the models of interest, and discuss the class of boundaries we consider. In Section IV, we explain the origin and meaning of topological entanglement entropy, and define the diagnostics used to detect boundary topological entanglement entropy. In Section V, we compute the entropy of bulk regions for Levin-Wen models. These computations are required for the Walker-Wang models, and provide a good warm-up. We then discuss the additional considerations for Walker-Wang models, and extend the computations to these. In Section VI, we compute the boundary entropy diagnostics for Levin-Wen models with boundary, followed by some classes of Walker-Wang models with boundary. We summarize in Section VII.

We include two appendices. In Appendix A, we provide proofs of some lemmas concerning (generalized) \mathcal{S} -matrices. In Appendix B, we provide proofs of some results concerning loop-gas models, and their entropies.

A. Summary of results

In Table I, we summarize our main results. Technical terms used in this summary are defined in Section II. The models we discuss will be introduced in the following sections, followed by the proofs of these results. We note that many of these results were previously known, for example the bulk Levin-Wen appears in Refs. 16 and 17. When the Levin-Wen model is defined by the fusion category $\mathbf{Vec}(G)$, the boundary LW results appear in Ref. 30. The bulk results for symmetric and modular Walker-Wang models appear in Ref. 28. We extend this to include all pointed inputs (all quantum dimensions equal to 1), as well as all input categories up to rank 5. This allows us to conjecture a general result. To the best of our knowledge, there are no results concerning boundary entropies of WW models beyond the 3D toric code [29].

Model	Bulk strings	Boundary algebra object	TEE
Levin-Wen	\mathcal{C} fusion	A	$\gamma = \log \mathcal{D}_{\mathcal{Z}(\mathcal{C})}^2$ $\Gamma = \log \mathcal{D}^2$
Walker-Wang	\mathcal{C} premodular	A	$\delta = \log \mathcal{D}_{\mathcal{Z}_2(\mathcal{C})}^2$ ^a $\Delta_\bullet = ?$ ^b
		$A = 1$	$\Delta_\circ = \log d_A^2 - \log \mathcal{D}^2 + \Delta_\bullet$ $\Delta_\bullet = \log \mathcal{D}^2$ $\Delta_\circ = 0$
Walker-Wang	\mathcal{C} symmetric	A	$\delta = \log \mathcal{D}_{\mathcal{Z}_2(\mathcal{C})}^2$ $\Delta_\bullet = \log \mathcal{D}^2 - \log d_A$ $\Delta_\circ = \log d_A$
Walker-Wang	\mathcal{C} pointed	A such that $A \cap \mathcal{Z}_2(\mathcal{C}) = \{1\}$ ^c	$\delta = \log \mathcal{D}_{\mathcal{Z}_2(\mathcal{C})}^2$ $\Delta_\bullet = \log \mathcal{D}^2 - 2 \log d_A$ $\Delta_\circ = 0$
		A such that $A \cap \mathcal{Z}_2(\mathcal{C}) = A$	$\Delta_\bullet = \log \mathcal{D}^2 - \log d_A$ $\Delta_\circ = \log d_A$

^a Conjectured, proven in many cases.

^b We do not have a general form at present.

^c Includes the case \mathcal{C} modular.

Table I: Summary of results, technical terms defined in Section II. The bulk strings are labeled by a unitary fusion category \mathcal{C} , possibly with extra structure. \mathcal{D} denotes the total quantum dimension of \mathcal{C} , A is an algebra object (with extra structure, see Section II) of dimension d_A , $\mathcal{Z}(\mathcal{C})$ and $\mathcal{Z}_2(\mathcal{C})$ are the Drinfeld and Müger centers of \mathcal{C} respectively.

II. PRELIMINARIES

Each of the physical models of interest in this work is defined by a collection of algebraic data. In the case of the (2+1)-dimensional models, this data can be conveniently packaged into a *fusion category*. In one higher dimension, additional data is required, so the package is a *premodular category*. Boundaries of these models can be specified using particular objects, called *algebra objects* in the input category.

In this section, we provide some (standard) definitions of these constructions, and introduce the notation we will use in the remainder of the manuscript. Many of the definitions that appear in this section are adapted from Ref. 31 and 32.

Throughout this work, we find it helpful to define a generalized Kronecker delta function. For this purpose, we use the indicator function $\delta_X = 1 \iff X = \text{true}$, and zero otherwise.

Definition 1 (Unitary spherical fusion category). *We sketch the definition of a unitary (skeletal) fusion category. For a more complete definition, we refer to Ref. 33, or for the physically minded reader Refs. 34 and 35. For our purposes, a unitary fusion category \mathcal{C} consists of:*

- A finite set of simple objects $\{1, a_1, a_2, \dots, a_k\}$, where 1 is the distinguished object called the unit.
- For each triple of simple objects $a, b, c \in \mathcal{C}$, a finite dimensional vector space $\mathcal{C}(a \otimes b, c)$, called a fusion space. The dimension of $\mathcal{C}(a \otimes b, c)$ defines the integer N_{ab}^c . For any simple objects a and b , fusion with the unit obeys $N_{1,a}^b = N_{a,1}^b = \delta_{a=b}$.
- Associator isomorphisms $(a \otimes b) \otimes c \cong a \otimes (b \otimes c)$
- To every object $a \in \mathcal{C}$, a dual object \bar{a} so that $\mathcal{C}(a \otimes \bar{a}, 1) \cong \mathbb{C} \cong \mathcal{C}(\bar{a} \otimes a, 1)$.

We refer to the integers N_{ab}^c as fusion rules. If all $N_{a,b}^c \in \{0, 1\}$, we call the category *multiplicity free*. The number of simple objects is called the *rank* of \mathcal{C} , denoted $\text{rk}(\mathcal{C})$. The unique positive solution to the set of equations

$$d_a d_b = \sum_c N_{ab}^c d_c \quad (1)$$

defines the quantum dimensions d_a of the simple objects. The total quantum dimension of \mathcal{C} is defined as

$$\mathcal{D}^2 := \sum_c d_c^2. \quad (2)$$

If all $d_a = 1$ (equivalently $\mathcal{D}^2 = \text{rk}(\mathcal{C})$), the category is called pointed. We remark that in the physics literature, this property is commonly called Abelian.

It is common to use a diagrammatic calculus of string diagrams to discuss fusion categories. Strings are labeled by objects from the category. If, in particular, a string is labeled by a simple object, it cannot change its labeling to another simple object except at a vertex, since there are no morphisms between distinct simple objects. Frequently, we neglect to draw strings labeled by the unit object for simplicity.

In string diagrams, the quantum dimensions are assigned to loops

$$a \circ = d_a, \quad (3)$$

and we refer to the insertion or removal of a loop as a loop move.

Once we choose a basis for $\mathcal{C}(a \otimes b, c)$, we denote a basis vector $\mu \in \mathcal{C}(a \otimes b, c)$ using a trivalent vertex[36]

$$\begin{array}{c} c \\ | \\ \mu \\ | \\ a \quad b \end{array} . \quad (4)$$

With these bases fixed, the associators can be expressed as unitary matrices

$$\begin{array}{c} d \\ | \\ e \quad \alpha \\ | \quad \backslash \\ a \quad b \quad c \end{array} = \sum_{(\mu, f, \nu)} \left[F_{abc}^d \right]_{(\alpha, e, \beta), (\mu, f, \nu)} \begin{array}{c} d \\ | \\ \mu \quad f \\ | \quad \backslash \\ a \quad b \quad c \end{array} , \quad (5)$$

with F_{abc}^d a unitary matrix for each valid choice of labels. This re-association is commonly referred to as an F -move. These matrices must obey the pentagon equations

$$\sum_{\delta} \left[F_{fcd}^e \right]_{(\alpha, g, \beta), (\delta, x, \rho)} \left[F_{abx}^e \right]_{(\delta, f, \gamma), (\mu, y, \nu)} = \sum_{\substack{(\sigma, z, \tau) \\ \varepsilon}} \left[F_{abc}^g \right]_{(\beta, f, \gamma), (\sigma, z, \tau)} \left[F_{azd}^e \right]_{(\alpha, g, \sigma), (\mu, y, \varepsilon)} \left[F_{bcd}^y \right]_{(\varepsilon, z, \tau), (\nu, x, \rho)}. \quad (6)$$

Additionally, the unit obeys the triangle equation [33], however we always, without loss of generality, choose the unit to be strict.

The category \mathcal{C} is equipped with a dagger structure, so we also have dual spaces to each fusion space. These are represented using upside-down vertices. We normalize the basis for $\mathcal{C}(a \otimes b, c)$ and $\mathcal{C}(c, a \otimes b)$ so that

$$\begin{array}{c} d \\ | \\ \nu \quad b \\ | \quad \backslash \\ a \quad \mu \\ | \\ c \end{array} = \delta_{c=d} \delta_{\mu=\nu} \sqrt{\frac{d_a d_b}{d_c}} \Bigg| c , \quad (7)$$

$$\left| \begin{array}{c} a \\ b \end{array} \right| = \sum_{c,\mu} \sqrt{\frac{d_c}{d_a d_b}} \left| \begin{array}{c} a \\ \mu \\ c \\ \mu \\ a \\ b \end{array} \right| . \quad (8)$$

All diagrams behave as though they were drawn on the surface of a sphere, for example

$$\left(\begin{array}{c} x \end{array} \right) = \left(\begin{array}{c} x \end{array} \right), \quad (9)$$

where x is any subdiagram.

We refer to Refs. 34 and 35 for a more detailed overview of these diagrams.

Definition 2 (Unitary braided fusion category). Given a unitary fusion category \mathcal{C} , a braiding is a map $a \otimes b \cong b \otimes a$, which is compatible with the associator of \mathcal{C} . Graphically, the braiding is encoded in the unitary R matrices

$$\left| \begin{array}{c} c \\ \mu \\ a \\ b \end{array} \right| = \sum_{\nu} \left[R_{ab}^c \right]_{\mu,\nu} \left| \begin{array}{c} c \\ \nu \\ a \\ b \end{array} \right| . \quad (10)$$

Compatibility with the (given) F matrices is encoded in the hexagon equations

$$\sum_{\gamma,\delta} \left[R_{ac}^e \right]_{\beta,\gamma} \left[F_{acb}^d \right]_{(\alpha,e,\gamma),(\sigma,f,\delta)} \left[R_{bc}^f \right]_{\delta,\tau} = \sum_{\substack{(\varepsilon,g,\rho) \\ \mu}} \left[F_{cab}^d \right]_{(\alpha,e,\beta),(\varepsilon,g,\rho)} \left[R_{gc}^d \right]_{\varepsilon,\mu} \left[F_{abc}^d \right]_{(\mu,g,\rho),(\sigma,f,\tau)} \quad (11)$$

$$\sum_{\gamma,\delta} \left[R_{ca}^e \right]_{\gamma,\beta}^* \left[F_{acb}^d \right]_{(\alpha,e,\gamma),(\sigma,f,\delta)} \left[R_{cb}^f \right]_{\tau,\delta}^* = \sum_{\substack{(\varepsilon,g,\rho) \\ \mu}} \left[F_{cab}^d \right]_{(\alpha,e,\beta),(\varepsilon,g,\rho)} \left[R_{cg}^d \right]_{\mu,\varepsilon}^* \left[F_{abc}^d \right]_{(\mu,g,\rho),(\sigma,f,\tau)} . \quad (12)$$

Definition 3 (Premodular category). In a braided fusion category, we can define twists θ_a by

$$\left| \begin{array}{c} \theta_a \\ a \\ a \end{array} \right| = \theta_a \left| \begin{array}{c} a \\ a \end{array} \right| . \quad (13)$$

If these twists obey the ribbon equations

$$\sum_{\nu} [R_{ba}^c]_{\mu,\nu} [R_{ab}^c]_{\nu,\rho} = \frac{\theta_c}{\theta_a \theta_b} \delta_{\mu=\rho}, \quad (14)$$

we call \mathcal{C} premodular.

In a premodular category, we can define the \mathcal{S} -matrix

$$\mathcal{S}_{a,b} := \frac{1}{D} \text{tr } B_{a,\bar{b}} = \frac{1}{D} \bar{a} \left(\begin{array}{c} \bar{b} \\ a \end{array} \right) b \quad (15)$$

$$= \frac{1}{D} \sum_x N_{a,\bar{b}}^x \frac{\theta_x}{\theta_a \theta_{\bar{b}}} d_x, \quad (16)$$

where

$$B_{a,b} := \text{Diagram} = \sum_{x,\mu} \sqrt{\frac{d_x}{d_a d_b}} \frac{\theta_x}{\theta_a \theta_b} \text{Diagram} . \quad (17)$$

For the results in this manuscript, it is important to understand which strings can be ‘uncrossed’. This is captured by the Müger center.

Definition 4 (Müger center [32]). *Let \mathcal{C} be a unitary premodular category. The symmetric or Müger center of \mathcal{C} is the full subcategory of \mathcal{C} with objects*

$$\mathcal{Z}_2(\mathcal{C}) := \{X \in \mathcal{C} \mid B_{X,Y} = \text{id}_{X \otimes Y} \forall Y \in \mathcal{C}\}. \quad (18)$$

A premodular category is symmetric if $\mathcal{Z}_2(\mathcal{C}) = \mathcal{C}$, and modular if $\mathcal{Z}_2(\mathcal{C}) = \mathbf{Vec}$. We will refer to premodular categories which are neither symmetric nor modular as properly premodular.

The \mathcal{S} -matrix acts as a witness for these properties. Symmetric categories have (matrix) rank 1 \mathcal{S} -matrices, while modular categories have invertible (unitary) \mathcal{S} -matrices.

It will be convenient to define a slight generalization of the \mathcal{S} -matrix.

Definition 5 (Connected \mathcal{S} -matrix). *Recall that the trivalent vertices define a vector space, with the μ labels indicating basis vectors. We can therefore define the operator \mathcal{S}_c by its action on the fusion space [34]*

$$\mathcal{S}_c = \frac{\sqrt{d_c}}{\mathcal{D}} \sum_x d_x \text{Diagram} . \quad (19)$$

The matrix elements of this operator are

$$[\mathcal{S}_c]_{(a,\alpha),(b,\beta)} = \frac{1}{\mathcal{D}} \bar{a} \text{Diagram} . \quad (20)$$

The usual \mathcal{S} -matrix is \mathcal{S}_1 . The connected \mathcal{S} -matrix is closely related to the punctured \mathcal{S} -matrix of Ref. 37.

The (connected) \mathcal{S} -matrix has a number of properties that we require.

Lemma 1. *Let \mathcal{C} be a unitary premodular category. The matrix elements of \mathcal{S} obey*

$$\frac{\mathcal{D}}{d_c} \mathcal{S}_{a,c} \mathcal{S}_{b,c} = \mathcal{S}_{a \otimes b, c} = \sum_x N_{a,b}^x \mathcal{S}_{x,c}. \quad (21)$$

Proof. Provided in Appendix A. □

Lemma 2. *Let \mathcal{C} be a unitary premodular category, then*

$$\sum_b d_b \mathcal{S}_{a,b} = \delta_{a \in \mathcal{Z}_2(\mathcal{C})} d_a \mathcal{D}, \quad (22)$$

where $\mathcal{Z}_2(\mathcal{C})$ is the Müger center.

Proof. Provided in Appendix A. \square

Corollary 1 (Premodular trap). *For any premodular theory, we have*

$$\left. \begin{array}{c} \text{Diagram: a circle with a vertical line through the center, labeled 'a' at the top and 'b' at the bottom.} \\ = \frac{\mathcal{S}_{a,\bar{b}}}{\mathcal{S}_{1,\bar{b}}} \end{array} \right| = \frac{\mathcal{D}\mathcal{S}_{a,\bar{b}}}{d_b}. \quad (23)$$

Using Lemmas 1 and 2, this gives

$$\frac{1}{\mathcal{D}^2} \sum_a d_a \left(\begin{array}{c} \text{Diagram: a circle with two vertical lines through the center, labeled 'a' at the top and 'x' and 'y' at the bottom.} \\ x \quad y \end{array} \right) = \sum_{z \in \mathcal{Z}_2(\mathcal{C}), \mu} \sqrt{\frac{d_z}{d_x d_y}} \left(\begin{array}{c} \text{Diagram: a tree with root 'z' branching to 'x' and 'y', with two mu labels on the edges.} \\ x \quad y \\ \mu_z \\ \mu_x \quad \mu_y \end{array} \right). \quad (24)$$

Lemma 3. *Let \mathcal{C} be a unitary premodular category, then*

$$\sum_{c \in \mathcal{C}} \text{Tr } \mathcal{S}_c^\dagger \mathcal{S}_c = \mathcal{D}^2, \quad (25)$$

where \mathcal{S}_c is the connected \mathcal{S} -matrix and \mathcal{D} is the total dimension of \mathcal{C} .

Proof. Provided in Appendix A. \square

Definition 6 (Algebra object). *An algebra (A, m, η) in a fusion category is an object $A = 1 \oplus a_1 \oplus a_2 \oplus \dots$, along with morphisms $m : A \times A \rightarrow A$ and $\eta : 1 \rightarrow A$. For simplicity, we restrict \mathcal{C} and A to be multiplicity free, that is each simple object a_i occurs at most once. We represent the multiplication morphism m as*

$$m = \begin{array}{c} A \\ \text{Diagram: a tree with root 'A' branching to two 'A' labels.} \\ A \quad A \end{array} = \sum_{a,b,c \in A} m_{ab}^c \begin{array}{c} c \\ \text{Diagram: a tree with root 'c' branching to 'a' and 'b'.} \\ a \quad b \end{array}. \quad (26)$$

To simplify the notation, we define $m_{xy}^z = 0$ whenever any of the labels do not occur in the decomposition of A . This allows us to always sum over simple objects in \mathcal{C} . Additionally, we suppress the A label. Any unlabeled lines carry an implicit A . The multiplication of the algebra should be associative (in \mathcal{C})

$$\begin{array}{c} \text{Diagram: a tree with root 'A' branching to two unlabeled lines.} \\ = \quad \begin{array}{c} \text{Diagram: a tree with root 'A' branching to two unlabeled lines.} \\ = \quad \begin{array}{c} \text{Diagram: a tree with root 'A' branching to two unlabeled lines.} \\ = \quad \dots \end{array} \end{array} \end{array}, \quad (27)$$

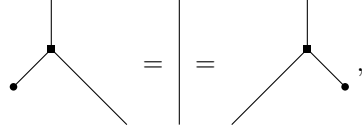
or in components

$$\sum_x m_{ab}^x m_{xc}^d \begin{array}{c} d \\ \text{Diagram: a tree with root 'd' branching to 'x', 'y', and 'z'.} \\ x \quad y \quad z \\ a \quad b \quad c \end{array} = \sum_y m_{ay}^d m_{bc}^y \begin{array}{c} d \\ \text{Diagram: a tree with root 'd' branching to 'x', 'y', and 'z'.} \\ x \quad y \quad z \\ a \quad b \quad c \end{array} = \sum_{x,z} m_{ab}^x m_{xc}^d \left[F_{abc}^d \right]_{xz} \begin{array}{c} d \\ \text{Diagram: a tree with root 'd' branching to 'x', 'y', and 'z'.} \\ x \quad y \quad z \\ a \quad b \quad c \end{array}, \quad (28)$$

where the final equality is obtained by using the F -move on the left hand side. The components of m therefore obey

$$m_{ay}^d m_{bc}^y = \sum_x m_{ab}^x m_{xc}^d \left[F_{abc}^d \right]_{xy}. \quad (29)$$

Multiplication by the unit obeys



$$(30)$$

or in components

$$\eta m_{1x}^x = 1 = \eta m_{x1}^x. \quad (31)$$

A coalgebra is the same, with everything flipped upside down.

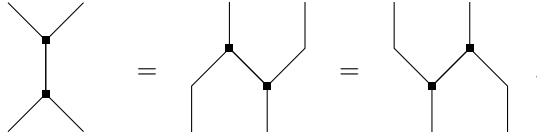
Two algebras (A, m, η) and (A, n, θ) are isomorphic if they can be related by

$$m_{ab}^c = n_{ab}^c \frac{\beta_c}{\beta_a \beta_b}, \quad (32)$$

$$\eta = \frac{1}{\beta_1} \theta, \quad (33)$$

where β_a are nonzero complex numbers. We can (and will) always use this to normalize $\eta = 1$. When it does not cause confusion, we will indicate an algebra by its object, for example $A = 1$, the ‘unit algebra’.

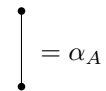
Definition 7 (Frobenius algebra). A Frobenius algebra is a quintuple $(A, m, \eta, \mu, \varepsilon)$, where (A, m, η) is an algebra, (A, μ, ε) is a coalgebra. The algebra and coalgebra maps obey



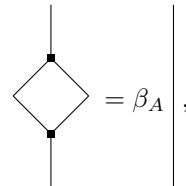
$$(34)$$

Since we only consider unitary \mathcal{C} , we require $\mu_c^{ab} = (m_{ab}^c)^*$.

A Frobenius algebra is said to be strongly separable if



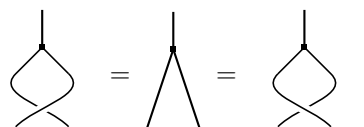
$$(35)$$



$$(36)$$

where $\alpha_A \beta_A \neq 0$. We normalize $\alpha_A = 1$ and $\beta_A = d_A$, where $d_A = \sum_{a \in A} d_a$.

If the underlying category \mathcal{C} is braided, we say the algebra A is commutative if



$$(37)$$

or in components

$$R_{ab}^c m_{ba}^c = m_{ab}^c = m_{ba}^c (R_{ba}^c)^*. \quad (38)$$

A. Examples

To aid understanding, and illustrate our results, we will refer to the following examples throughout the remainder of the manuscript.

The unitary fusion category $\mathbf{Vec}^\omega(\mathbb{Z}_2)$ is the category of finite dimensional \mathbb{Z}_2 -graded vector spaces. The simple objects are labeled by the group elements $\mathbb{Z}_2 := \{1, x \mid x^2 = 1\}$. Since we neglect to draw the unit object, corresponding to the identity group element, the only nonzero trivalent vertex is

$$\begin{array}{c} \diagup \\ \diagdown \end{array} . \quad (39)$$

These are pointed categories, and so $d_x = 1$. The total quantum dimension is $\mathcal{D}^2 = 2$.

It is straightforward to check that there are exactly two inequivalent associators compatible with this fusion rule, namely

$$\begin{array}{c} \diagup \\ \diagdown \end{array} = \omega \begin{array}{c} \diagdown \\ \diagup \end{array} , \quad (40)$$

with $\omega = \pm 1$. With the associator fixed, there are two compatible braidings

$$\begin{array}{c} \text{---} \\ \text{---} \end{array} = \varphi \begin{array}{c} \diagup \\ \diagdown \end{array} , \quad (41)$$

with $\varphi^2 = \omega$. The twists and \mathcal{S} -matrices of these models are given by

$$\theta_x = \varphi \quad \mathcal{S} = \frac{1}{\sqrt{2}} \begin{pmatrix} 1 & 1 \\ 1 & \omega \end{pmatrix}, \quad (42)$$

so the categories are modular when $\omega = -1$, and symmetric when $\omega = +1$. We denote by $\mathbf{Vec}^{\omega,\varphi}(\mathbb{Z}_2)$ the braided category, with associator ω and braiding φ .

These four examples are included in the attached Mathematica file [38] as $\mathbf{Vec}^{1,1}(\mathbb{Z}_2) = \mathbf{FR}_{1;0}^{2,0}$, $\mathbf{Vec}^{1,-1}(\mathbb{Z}_2) = \mathbf{FR}_{1;2}^{2,0}$, $\mathbf{Vec}^{-1,i}(\mathbb{Z}_2) = \mathbf{FR}_{1;1}^{2,0}$, and $\mathbf{Vec}^{-1,-i}(\mathbb{Z}_2) = \mathbf{FR}_{1;3}^{2,0}$.

For these examples, there are two possible algebras, namely $A_0 := 1$, with trivial m morphism, and $A_1 := 1 \oplus x$. The algebra A_0 is compatible as a commutative algebra. For A_1 , compatibility as a Frobenius algebra (Eq. (29)) reduces to

$$m_{x,x}^1 \omega = m_{x,x}^1, \quad (43)$$

so is only a valid algebra object when $\omega = 1$. In that case, A_1 is commutative when

$$m_{x,x}^1 \varphi = m_{x,x}^1 \iff \varphi = 1. \quad (44)$$

III. LOOP-GAS MODELS IN TWO AND THREE DIMENSIONS

In this work, we study loop-gas models. In their most general form, these models have ground states described by superpositions of string diagrams subject to a collection of rules, for example a diagram may be declared invalid in a ground state superposition if it contains an ‘open string’. We focus on topological loop-gas models. In this case, the rules are a collection of local manipulations or moves that states must be invariant under. These are designed to ensure invariance under diffeomorphism. Given a triangulation of the manifold, which provides a lattice structure on which a condensed matter model can be defined [39], the local moves ensure retriangulation invariance.

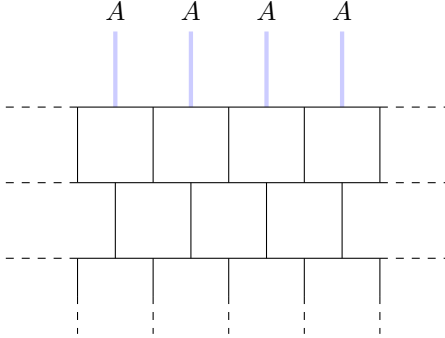


Figure 1: An algebra specifies a boundary for a Levin-Wen model on a ‘comb lattice’. Dashed lines indicate the lattice continues. The top, thick blue lines are labeled by an algebra A that defines a physical boundary to the lattice.

Levin-Wen [4, 9] (LW) and Walker-Wang [10, 40–42] (WW) models are, respectively, two- and three- dimensional Hamiltonian models that give rise to topological loop-gas states as their ground states. Hamiltonians for these models are given in Ref. 9 and Ref. 10 for LW and WW models respectively. Our results do not depend on the particular form of the Hamiltonian, rather on universal properties of the ground states in the associated topological phase.

Quasiparticle excitations in these models are defects in the ground state, corresponding to a local change in the rules. Far from the excitations, the excited state remains invariant under the original moves but, for example, a string may be allowed to terminate at the location of the excitation.

A. Bulk

Given a unitary spherical fusion category \mathcal{C} (Definition 1), and a given lattice embedded on a 2 dimensional manifold, the ground states of LW models are superpositions of closed diagrams from the category. Strings lie along the edges of the lattice, and closed means they cannot terminate. On the lattice, the string types correspond to states of a qudit with dimension equal to the rank of \mathcal{C} . At the vertices, the fusion rules of the category dictate which strings can fuse.

If a given configuration occurs in a particular ground state, then any other configuration that is obtainable by local moves (i.e. F - or loop-moves) also occurs in that ground state. The relative coefficients are dictated by the F -symbols, and consistency is ensured by the pentagon equation. Since the allowed moves are all local, there may be multiple ground states on manifolds with nontrivial genus. For example, a loop enclosing a cycle of the torus cannot be removed with the local loop move.

The collection of excitations (anyons) resulting from the Levin-Wen construction is called the Drinfeld center, denoted $\mathcal{Z}(\mathcal{C})$. We refer to Ref. 33 for a formal definition.

In (3+1)-dimensions, for WW models, the diagrams can also include crossings. This required additional data to be added to the category, in particular a braiding (Definition 2). If we picture these diagrams embedded in 3 dimensional space, there is an ambiguity involved in these crossing. For example, if we look at a crossing from ‘the side’, there is no crossing. This ambiguity can be resolved by widening the strings into ribbons. This is implemented by insisting that the braided category is premodular (Definition 3).

Given a premodular category \mathcal{C} , and a lattice embedded in a 3D manifold, a WW model is defined in essentially the same way as a LW model. In addition to the F - and loop- moves, R - moves and insertion of links (or knots), such as the \mathcal{S} -matrix are allowed. Again, given any closed string configuration, any other configuration that can be reached via these rules is included in the ground state superposition.

Within the collection of string types, the subset that can be ‘unlinked’ from any other string is called the Müger center of \mathcal{C} , denoted $\mathcal{Z}_2(\mathcal{C})$ (Definition 4). The Müger center labels the particle excitations of the Walker-Wang model [43].

B. Boundaries

To include a physical boundary in a loop-gas model, the rules must be modified. For the topological loop-gas models, these rules are again defined by local moves in the vicinity of the boundary. These must be compatible

with the bulk moves, and ensure topological/retriangulation invariance at the boundary. We restrict our attention to gapped boundaries.

There are various equivalent classifications for the gapped boundaries of Levin-Wen models [11, 12, 44–47]. In this work, we use an internal classification. In this framework, gapped boundary conditions for Levin-Wen models are labeled by indecomposable strongly separable, Frobenius algebra objects (Definition 7) in \mathcal{C} up to Morita equivalence [11, 12]. We restrict to multiplicity free algebras for simplicity. These algebra objects are (not necessarily simple) objects in \mathcal{C} , and their simple subjects are roughly the string types that are allowed to terminate on the boundary.

On the comb lattice (Fig. 1), for example, the dangling edges only take values in the chosen algebra. Far from the boundary, the ground states look just like those with no boundary. Near the boundary, loops are no longer required to be closed, rather they can terminate on the boundary if their label occurs within the algebra. We refer to Refs. 11 and 12 for more details, including an explicit Hamiltonian.

Just as in the bulk, when we move to (3+1)-dimensions, the braiding must be taken into account. A general classification of gapped boundaries for Walker-Wang models has not been established, so we proceed for a class of boundaries generalizing those for Levin-Wen introduced above. As before, a boundary is labeled by an algebra object. Since the bulk is braided, an additional compatibility condition is required, namely that the algebra is commutative (Eq. (37)). Finally, in this work, an indecomposable, strongly separable, commutative, Frobenius algebra object labels a gapped boundary condition of a Walker-Wang model [48].

C. Examples

Recall the examples from Section II A. In (2+1)-dimensions, $\mathbf{Vec}^{1,\pm 1}(\mathbb{Z}_2)$ lead to the same loop-gas model, since the LW construction doesn't make use of the braiding. This model is the equally weighted superposition of all loop diagrams (with no branching due to the fusion rules). This is the ground state of the toric code model [5].

Likewise, $\mathbf{Vec}^{\pm i}(-1)$ correspond to the same loop-gas model. Due to the nontrivial Frobenius-Schur indicator [34], it is convenient to associate -1 to a loop rather than $+1$ (otherwise we can take extra care when bending lines). The ground state is therefore a superposition of loops, but weighted by $(-1)^{\text{number of loops}}$. This is commonly called the double-semion model.

There are two possible (gapped) boundaries for the toric code, the ‘smooth’ boundary, corresponding to the algebra A_0 , and the ‘rough’ boundary, corresponding to A_1 . We refer to Ref. 49 for more details. The double-semion model only allows for one kind of (gapped) boundary, labeled by A_0 .

In (3+1)-dimensions, each of these models labels a distinct WW model. The models $\mathbf{Vec}^{1,1}(\mathbb{Z}_2)$, $\mathbf{Vec}^{1,-1}(\mathbb{Z}_2)$ are commonly called the bosonic- and fermionic- toric code models respectively [26, 50]. Since these categories both have $\mathcal{Z}_2(\mathcal{C}) = \{1, x\}$, they both have a single particle excitation, in addition to the trivial excitation, whose self-statistics lead to the names of the models. The two models $\mathbf{Vec}^{\pm i}(-1)$ are both referred to as semion models.

In (3+1)-dimensions, the bosonic toric code still has two kinds of boundaries, but the remaining models are only compatible with the trivial boundary labeled by A_0 .

IV. ENTROPY DIAGNOSTICS

In what follows we describe the universal correction to the area law that we expect for topological phases. We then define two diagnostics that can be used to probe the properties of the excitations at the boundary of three-dimensional topological phases.

A. The universal correction to the area law

The ground states of topological phases of matter demonstrate robust long-range entanglement that is not present in trivial phases [15–17]. Typically, we expect the entanglement entropy shared between a subsystem of a ground state of a gapped phase with the rest of the system to respect an area law, i.e., the entanglement will scale with the size of the surface area of the subsystem. The long-range entanglement manifests as a universal correction to the area law. More precisely, we expect that if we partition the ground state of a system into two subsystems, R and its complement R^c , the entanglement entropy, S_R , will satisfy

$$S_R = \alpha |\partial R| - b_R \gamma. \quad (45)$$

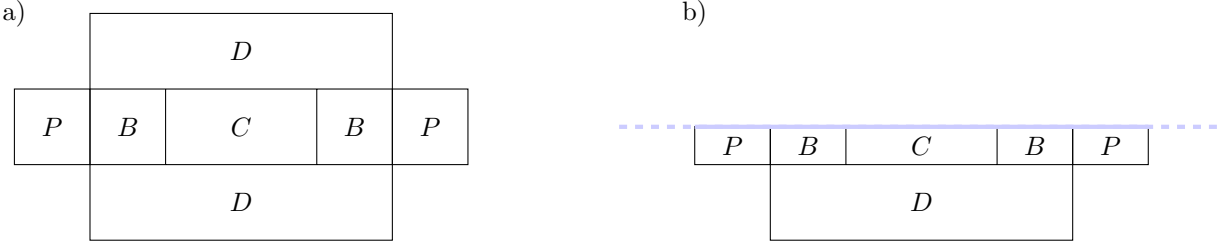


Figure 2: Example of subsystems that can be used to find topological entropies in 2D. The region A is the complement of BCD . The regions a) are used to find the bulk entropy γ , and the regions b) are used for the boundary entropy Γ .

Here α is a non-universal coefficient that depends on the microscopic details of the system, $|\partial R|$ is the surface area of the interface between the partitioned regions, b_R is the number of disjoint components of the interface between R and R^c , and γ is a universal constant commonly known as the topological entanglement entropy (TEE). We have assumed that R is large compared to the correlation length of the system, and its shape has no irregular features.

B. Two-dimensional models

Intimately connected to the long-range entanglement of a topological phase are the properties of its low-energy excitations. A large class of topological models in two-dimensions are the Levin-Wen (LW) string-net models [9]. These models support topological point-like excitations that can be braided to change the state of the system.

Throughout this work we will be interested in the boundaries of topological phases. Importantly, topological particles can behave differently in the vicinity of the boundary of a phase. For instance, topological particles found in the bulk may become trivial particles close to certain boundaries. This is because topological particles can condense at the boundary. We therefore see that the nature of some particles can change depending on whether they are in the vicinity of a boundary.

As the physics of quasi-particles of a topological phase can change close to its boundary, so to do we expect that the nature of its long-range entanglement to change. In Ref. 29, several topological entanglement entropy diagnostics were found to probe long-range entanglement of a model, both in the bulk and near to a boundary. The first is the bulk topological entanglement entropy

$$\gamma := S_{BC} + S_{CD} - S_B - S_D, \quad (46)$$

where the regions are depicted in Fig. 2a, and $XY := X \cup Y$. If $\gamma = 0$, all point-like excitations can be created on the distinct parts of P with a creation operator that has no support on ACD , where A is the region that is complement to those shown in the figure. In this case, we declare them trivial. Conversely, if there are non-trivial topological excitations, for example created with string-like operators, γ is necessarily non-zero.

In the presence of a gapped boundary, the excitations may differ. If a bulk topological excitation can be discarded or ‘condensed’ on the boundary, it is possible to locally create such an excitation near the boundary. This is detected using the diagnostic

$$\Gamma := S_{BC} + S_{CD} - S_B - S_D, \quad (47)$$

where the regions are depicted in Fig. 2b. If $\Gamma = 0$, all point-like excitations on P can be created with an operator that has no support on ACD , while non-trivial excitations require non-zero Γ .

C. Three-dimensional models

A natural generalization of Levin-Wen models to three dimensions is the class called Walker-Wang (WW) models [10]. These models give rise to both point- and line-like topological particles in the bulk, in addition to boundary excitations. Unlike Levin-Wen models, in some instances topological particles are only found at the boundary.

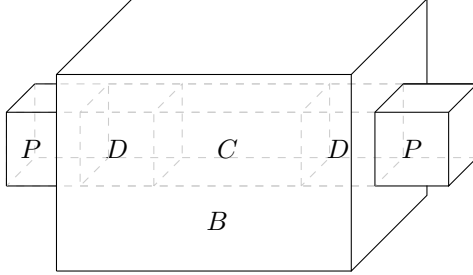


Figure 3: Partitioning of the lattice for detecting excitations in the bulk. B encircles CD , and A is the complement of BCD . If δ is small, excitations on P can be created by only acting on PD and so have trivial statistics.

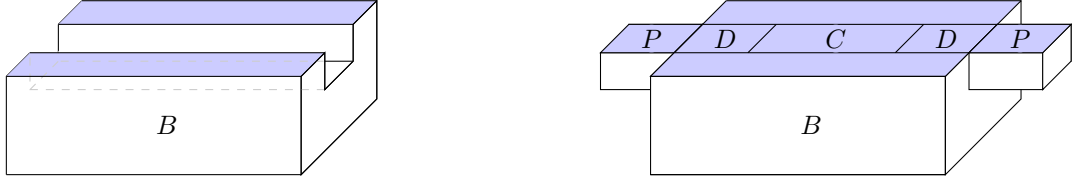


Figure 4: Partitioning of the lattice for detecting point-like excitations on the boundary. The top (blue) surface is on the physical boundary of the lattice. If Δ_\bullet is small, excitations on P can be created by only acting on PD and so have trivial statistics.

Since there are two kinds of topological excitations in 3D, we might expect that there are two bulk diagnostics generalizing γ . However, as it has been shown [25, 28], these coincide. We define the bulk topological entanglement entropy

$$\delta := S_{BC} + S_{CD} - S_B - S_D, \quad (48)$$

where the regions are depicted in Fig. 3. We obtained this choice of region following intuition given in Ref. [29] where we consider the creating point excitations at the distinct parts of region P using a string operator supported on ACD . We find δ is zero only if all the excitations can be created using an operator with local support. The boundary diagnostics that we describe next are obtained by bisecting the regions shown in Fig. 3 along different planes where the boundary lies.

In Ref. [29] two topological entanglement entropy diagnostics were found to probe long-range entanglement of a model near to a boundary. The first boundary diagnostic is an indicator that point-like topological particles can be created at the boundary of the system, and the second indicates that the boundary supports extended one-dimensional ‘loop-like’ topological particles. Unlike in the bulk, these diagnostics do not necessarily coincide. The first

$$\Delta_\bullet := S_{BC} + S_{CD} - S_B - S_D, \quad (49)$$

defined using the regions in Fig. 4, is non-zero if non-trivial point-like excitations can be created near the boundary. If $\Delta_\bullet = 0$, all point-like excitations on P can be created with a local operator, so they are necessarily trivial. Conversely, if there are non-trivial point-like particles near the boundary, $\Delta_\bullet > 0$.

The final diagnostic is designed to detect nontrivial loop-like excitations. Using the regions depicted in Fig. 5, this diagnostic is

$$\Delta_\circ := S_{BC} + S_{CD} - S_B - S_D. \quad (50)$$

Similarly to the other diagnostics, if Δ_\circ is zero, then line-like excitations must be trivial. Conversely, Δ_\circ must be nonzero if non-trivial loop excitations can be created at the boundary.

The diagnostics presented in Ref. 29 were found using generic arguments about the support of deformable operators that are used to create excitations. As such, it was shown rigorously that the null outcome is obtained only if a boundary does not give rise to topological particles. Conversely, a boundary that gives rise to topological excitations must give a positive reading for these diagnostics. However, due to spurious contributions [51–55], the generic arguments cannot guarantee that the diagnostics do not give false positives and, moreover, the work gives no interpretation for the

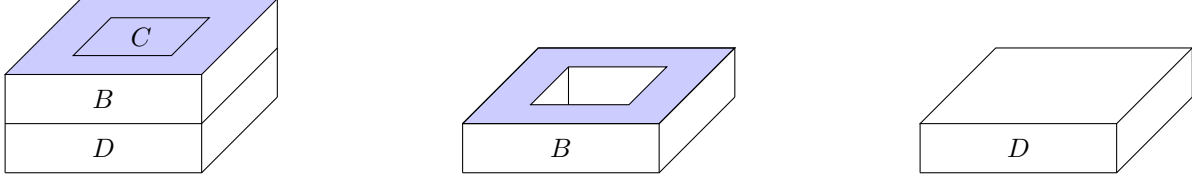


Figure 5: Partitioning of the lattice for detecting line-like excitations on the boundary. The top (blue) surface is on the boundary of the lattice. If Δ_\circ is small, excitations on B can be created without acting on C and so have trivial statistics.

magnitude of a positive reading. In our work, we restrict to loop-gas models. In that setting, for a large class of models, we obtain expressions for the topological entanglement entropy near the boundary.

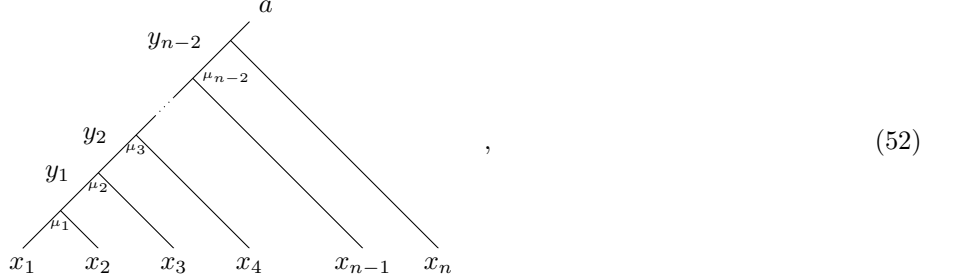
V. BULK ENTROPY OF TOPOLOGICAL LOOP-GASSES

We now show how the entanglement entropy of ground states of Levin-Wen models is computed far from any boundary, before moving on to Walker-Wang models. To make the calculation we take the Schmidt decomposition of the ground state

$$|\psi\rangle = \sum_{\lambda=1}^r \Phi_\lambda |\psi_R^\lambda\rangle |\psi_{R^c}^\lambda\rangle, \quad (51)$$

for regions R , where the sets $\{|\psi_R^\lambda\rangle\}$ and $\{|\psi_{R^c}^\lambda\rangle\}$ are orthonormal, and r is the Schmidt rank of the state $|\psi\rangle$. This allows us to compute the reduced state ρ_R on R . Diagonalizing this matrix yields the entanglement entropy.

For the following, we will need several results concerning fusion trees. Consider fusing n strings labeled $\vec{x} := (x_1, x_2, \dots, x_n)$ to a fixed object a . Using F -moves, we can bring the fusion tree for this process into the canonical form



where $1 \leq \mu \leq N_{a,b}^c$ parameterizes the distinct fusion channels $a \otimes b \rightarrow c$. In the following, sums over x_i , y_i are over all simple objects in \mathcal{C} . First, we need two results concerning summing over trees.

Lemma 4. *Let \mathcal{C} a unitary fusion category, then for a fixed simple fusion outcome a ,*

$$\sum_{\vec{x}, \vec{y}} N_{x_1 x_2}^{y_1} N_{y_1 x_3}^{y_2} \dots N_{y_{n-2} x_n}^a \prod_{j \leq n} d_{x_j} = d_a \mathcal{D}^{2(n-1)}, \quad (53)$$

where $\mathcal{D} = \sqrt{\sum_i d_i^2}$ is the total quantum dimension of \mathcal{C} .

Proof. Provided in Appendix B. □

Lemma 5. *Let \mathcal{C} a unitary fusion category, then for a fixed simple fusion outcome a ,*

$$\sum_{\vec{x}, \vec{y}} N_{x_1 x_2}^{y_1} N_{y_1 x_3}^{y_2} \dots N_{y_{n-2} x_n}^a \frac{\prod_{j \leq n} d_{x_j}}{\mathcal{D}^{2(n-1)}} \log \prod_{k \leq n} d_{x_k} = n d_a \sum_x \frac{d_x^2 \log d_x}{\mathcal{D}^2}. \quad (54)$$

Proof. Provided in Appendix B. \square

Finally, we need the probability of a given fusion tree in a topological loop-gas model.

Lemma 6 (Probability of trees). *Let \mathcal{C} a unitary fusion category. Given a fusion outcome a on n edges, the probability of the tree in Eq. (52) is*

$$\Pr[\vec{x}, \vec{y}, \vec{\mu} | a] = \frac{\prod_{j \leq n} d_{x_j}}{d_a \mathcal{D}^{2(n-1)}}. \quad (55)$$

Proof. Provided in Appendix B. \square

Throughout the remainder of this section, we use the following condensed notation

$$\sum_{\vec{x}, \vec{y}, \vec{\mu}} := \sum_{x_1, \dots, x_n} \sum_{y_1, \dots, y_{n-2}} \sum_{\mu_1, \dots, \mu_{n-2}} \quad (56)$$

$$= \sum_{x_1, \dots, x_n} \sum_{y_1, \dots, y_{n-2}} N_{x_1 x_2}^{y_1} N_{y_1 x_3}^{y_2} \dots N_{y_{n-2} x_n}^a, \quad (57)$$

where we frequently leave the fusion outcome a implicit.

A. Levin-Wen models

Theorem 1 (Topological entropy of (2+1)D Levin-Wen models in the bulk [16, 17, 56]).

Consider the regions shown in Fig. 2a, then the Levin-Wen model defined by a unitary spherical fusion category \mathcal{C} , with total dimension \mathcal{D} , has topological entropy

$$\gamma = 2 \log \mathcal{D}^2 = \log \mathcal{D}_{\mathcal{Z}(\mathcal{C})}^2, \quad (58)$$

where $\mathcal{Z}(\mathcal{C})$ is the modular category called the Drinfeld center [33] of \mathcal{C} which describes the anyons of the theory.

Examples. Recall the examples from Section II A. As discussed in Section III C, these label two distinct loop-gas models in (2+1)-dimensions, the toric code and double semion models. Since all the input categories for these examples have $\mathcal{D}^2 = 2$, the TEE is $\gamma = 2 \log 2$ for both.

Lemma 7 (Entropy of (union of) simply connected bulk regions [17, 28, 56]). *On a region R in the bulk consisting of the disjoint union of simply connected sub-regions, the entropy is*

$$S_R = n S[\mathcal{C}] - b_0 \log \mathcal{D}^2, \quad (59)$$

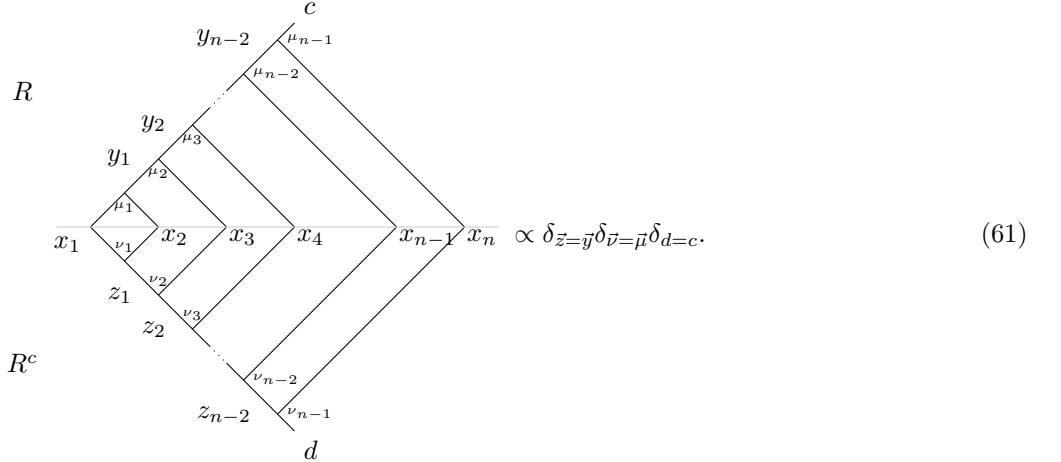
where b_0 is the number of disjoint interface components of R , n is the number of links crossing the entanglement interface, and

$$S[\mathcal{C}] := \log \mathcal{D}^2 - \sum_x \frac{d_x^2 \log d_x}{\mathcal{D}^2}. \quad (60)$$

Proof. Consider a ball R with n sites along the interface, in the configuration $\vec{x} = x_1, x_2, \dots, x_n$. Since any configuration must be created by inserting closed loops into the empty state, the total ‘charge’ crossing the interface must be 1. For a fixed \vec{x} , there are now many ways for this to happen, parameterized by trees depicted in Eq. (52) with fusion outcome $a = 1$.

Trees with distinct labelings (in \vec{x} , \vec{y} or $\vec{\mu}$) are orthogonal. This means that if the tree Eq. (52) occurs adjacent to

the interface within R , it must also occur on the other side of the interface



If the trees on either side of the cut had different branching structures, we could use local moves on either side of the cut to bring them to this standard form.

We take the Schmidt decomposition of the ground state as follows

$$|\psi\rangle = \sum_{\vec{x}, \vec{y}, \vec{\mu}} \Phi_{\vec{x}, \vec{y}, \vec{\mu}} |\psi_R^{\vec{x}, \vec{y}, \vec{\mu}}\rangle |\psi_{R^c}^{\vec{x}, \vec{y}, \vec{\mu}}\rangle, \quad (62)$$

where the notation $\vec{x}, \vec{y}, \vec{\mu}$ indicates the labeling of a valid tree as in Eq. (52). The state $|\psi_R^{\vec{x}, \vec{y}, \vec{\mu}}\rangle$ includes any state that can be reached from Eq. (52) (with $a = 1$) by acting only on R . The reduced state on R is

$$\rho_R = \sum_{\vec{x}, \vec{y}, \vec{\mu}} |\Phi_{\vec{x}, \vec{y}, \vec{\mu}}|^2 |\psi_R^{\vec{x}, \vec{y}, \vec{\mu}}\rangle \langle \psi_R^{\vec{x}, \vec{y}, \vec{\mu}}| \quad (63)$$

$$= \sum_{\vec{x}, \vec{y}, \vec{\mu}} \Pr[\vec{x}, \vec{y}, \vec{\mu}|1] |\psi_R^{\vec{x}, \vec{y}, \vec{\mu}}\rangle \langle \psi_R^{\vec{x}, \vec{y}, \vec{\mu}}|, \quad (64)$$

where $\Pr[\vec{x}, \vec{y}, \vec{\mu}|1]$ is the probability of the labeled tree, given that \vec{x} fuses to 1. From Lemma 6, the reduced state is

$$\rho_R = \sum_{\vec{x}, \vec{y}, \vec{\mu}} \frac{\prod_{j \leq n} d_{x_j}}{\mathcal{D}^{2(n-1)}} |\psi_R^{\vec{x}, \vec{y}, \vec{\mu}}\rangle \langle \psi_R^{\vec{x}, \vec{y}, \vec{\mu}}|. \quad (65)$$

The von Neumann entropy of ρ_R is therefore

$$S_R := -\text{tr} \rho_R \log \rho_R \quad (66)$$

$$= - \sum_{\vec{x}, \vec{y}, \vec{\mu}} \frac{\prod_{j \leq n} d_{x_j}}{\mathcal{D}^{2(n-1)}} \log \frac{\prod_{k \leq n} d_{x_k}}{\mathcal{D}^{2(n-1)}} \quad (67)$$

$$= \frac{\log \mathcal{D}^{2(n-1)}}{\mathcal{D}^{2(n-1)}} \sum_{\vec{x}, \vec{y}, \vec{\mu}} \prod_{j \leq n} d_{x_j} - \sum_{\vec{x}, \vec{y}, \vec{\mu}} \frac{\prod_{j \leq n} d_{x_j}}{\mathcal{D}^{2(n-1)}} \log \prod_{k \leq n} d_{x_k} \quad (68)$$

$$= n(\log \mathcal{D}^2 - \sum_x \frac{d_x^2 \log d_x}{\mathcal{D}^2}) - \log \mathcal{D}^2 \quad (69)$$

$$= nS[C] - \log \mathcal{D}^2 \quad (70)$$

where Lemmas 4 and 5 are applied to the left and right terms of line (68), respectively, and

$$S[C] := \log \mathcal{D}^2 - \sum_x \frac{d_x^2 \log d_x}{\mathcal{D}^2}. \quad (71)$$

It is straightforward to check that this holds on each sub-region of R . \square

Applying Lemma 7 to the regions in Fig. 2a completes the proof of Theorem 1.

B. Walker-Wang models

In this section, we prove the following result for the bulk diagnostic for Walker-Wang models. The essential arguments in this section were made in Ref. 28, however we use slightly different language that allows the result to be applied more generally.

Theorem 2. *For a Walker-Wang model defined by a unitary premodular category \mathcal{C} , the topological entanglement entropy (defined using the regions in Fig. 3) in the bulk is given by*

$$\delta = \sum_{c, \lambda_c} \frac{\lambda_c}{\mathcal{D}^2} \log \frac{\lambda_c}{d_c}, \quad (72)$$

where $\{\lambda_c\}$ are the eigenvalues of $\mathcal{S}_c^\dagger \mathcal{S}_c$, and \mathcal{S}_c is the connected \mathcal{S} -matrix (Definition 5).

Proof. In simply connected regions, the arguments from Lemma 7 still hold. The other type of region in Fig. 2a is a torus. In this case, we cannot simply decompose the ground state as in Eq. (62), with the sum over configurations on the interface. Recall that the reason we could do this for a simple region was ground states are created by inserting closed loops, and all closed loops except those crossing the interface can be added entirely within either R or R^c . This is not the case for a toroidal region. Consider, for example, the configuration depicted in Fig. 6. The closed string inside R (red, dashed) cannot be altered by acting entirely within R , so contributes additional entanglement to the ground state, which is not witnessed by the interface configuration. Additionally, the two loops may be connected by a string, such that the global charge is trivial. Therefore, unlike for simply connected regions, the net charge crossing the boundary is not necessarily trivial. With these considerations, we can decompose the ground state as

$$|\psi\rangle = \sum_{\substack{\vec{x}, \vec{y}, \vec{\mu} \\ c, a, \alpha, b, \beta}} \Phi_{\vec{x}, \vec{y}, \vec{\mu}, c} \frac{[\mathcal{S}_c]_{(b, \beta)(a, \alpha)}}{\mathcal{D}} |\psi_R^{\vec{x}, \vec{y}, \vec{\mu}, c, a, \alpha}\rangle |\psi_{R^c}^{\vec{x}, \vec{y}, \vec{\mu}, c, b, \beta}\rangle, \quad (73)$$

where \mathcal{S}_c is the connected \mathcal{S} -matrix defined in Eq. (20). The indices $\vec{x}, \vec{y}, \vec{\mu}$ are as in Eq. (62), b labels the loop encircling R , while a is the loop within R , and c is the total charge crossing the boundary (the top label in Eq. (52)). The reduced state on R is

$$\rho_R = \sum_{\substack{\vec{x}, \vec{y}, \vec{\mu} \\ a_1, \alpha_1, a_2, \alpha_2, c}} \frac{\text{Pr}[\vec{x}, \vec{y}, \vec{\mu}|c]}{\mathcal{D}^2} [\mathcal{S}_c^\dagger \mathcal{S}_c]_{(a_2, \alpha_2)(a_1, \alpha_1)} |\psi_R^{\vec{x}, \vec{y}, \vec{\mu}, a_1, \alpha_1, c}\rangle \langle \psi_R^{\vec{x}, \vec{y}, \vec{\mu}, a_2, \alpha_2, c}| \quad (74)$$

$$= \sum_{\substack{\vec{x}, \vec{y}, \vec{\mu} \\ a_1, \alpha_1, a_2, \alpha_2, c}} \frac{\prod_{j \leq n} d_{x_j}}{d_c \mathcal{D}^{2n}} [\mathcal{S}_c^\dagger \mathcal{S}_c]_{(a_2, \alpha_2)(a_1, \alpha_1)} |\psi_R^{\vec{x}, \vec{y}, \vec{\mu}, a_1, \alpha_1, c}\rangle \langle \psi_R^{\vec{x}, \vec{y}, \vec{\mu}, a_2, \alpha_2, c}|. \quad (75)$$

To compute the entropy of this state, it is convenient to diagonalize it. Denote the eigenvalues of $\mathcal{S}_c^\dagger \mathcal{S}_c$ by $\{\lambda_c\}$. By a unitary change of basis, we have

$$U \rho_R U^\dagger = \sum_{\substack{\vec{x}, \vec{y}, \vec{\mu}, \\ c, \lambda_c}} \frac{\prod_{j \leq n} d_{x_j}}{d_c \mathcal{D}^{2n}} \lambda_c |\varphi_{\lambda_c}^{\vec{x}, \vec{y}, \vec{\mu}, c}\rangle \langle \varphi_{\lambda_c}^{\vec{x}, \vec{y}, \vec{\mu}, c}|, \quad (76)$$

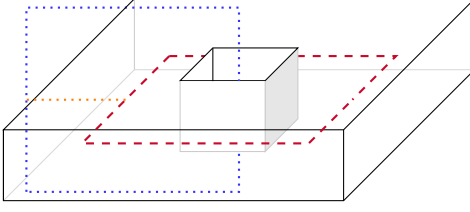


Figure 6: When the region R is not simply connected, the computation of entropy is more subtle. There is additional entanglement in the system due to intersecting loops that cannot be created in R or R^c separately. This is not witnessed by the configuration of strings on the interface.

with von Neumann entropy

$$S_R = nS[\mathcal{C}] - \sum_{c, \lambda_c} \frac{\lambda_c}{\mathcal{D}^2} \log \frac{\lambda_c}{d_c}, \quad (77)$$

where Lemmas 3 to 5 are used. Combining with Lemma 7 completes the proof. \square

Conjecture 1. Let \mathcal{C} be a unitary premodular category \mathcal{C} , and define the connected \mathcal{S} -matrix via its matrix elements

$$[\mathcal{S}_c]_{(a, \alpha), (b, \beta)} = \frac{1}{\mathcal{D}} \bar{a} \left(\begin{array}{c} c \\ \alpha \\ \bar{b} \end{array} \right) \left(\begin{array}{c} a \\ \beta \\ b \end{array} \right) \bar{c}. \quad (78)$$

The connected \mathcal{S} -matrix obeys

$$\sum_{c, \lambda_c} \frac{\lambda_c}{\mathcal{D}^2} \log \frac{\lambda_c}{d_c} = \log \mathcal{D}_{\mathcal{Z}_2(\mathcal{C})}^2, \quad (79)$$

where $\{\lambda_c\}$ are the eigenvalues of $\mathcal{S}_c^\dagger \mathcal{S}_c$, and $\mathcal{Z}_2(\mathcal{C})$ is the Müger center of \mathcal{C} .

We conjecture that Eq. (79) holds in general, however we are currently unable to compute the spectrum of \mathcal{S}_c beyond the families outlined in Theorem 3.

Theorem 3. For a Walker-Wang model defined by a unitary premodular category of one of the following types:

- $\mathcal{C} = \mathcal{A} \boxtimes \mathcal{B}$, where \mathcal{A} is symmetric and \mathcal{B} is modular [28],
- \mathcal{C} pointed,
- $\text{rk}(\mathcal{C}) < 6$ and multiplicity free,
- $\text{rk}(\mathcal{C}) = \text{rk}(\mathcal{Z}_2(\mathcal{C})) + 1$ and $d_x = \mathcal{D}_{\mathcal{Z}_2(\mathcal{C})}$, where x is the additional object (as a special case, \mathcal{C} is a Tambara-Yamagami category [57, 58]),

then Eq. (79) holds. As a consequence, the topological entanglement entropy (defined using the regions in Fig. 3) in the bulk is given by

$$\delta = \log \mathcal{D}_{\mathcal{Z}_2(\mathcal{C})}^2, \quad (80)$$

where $\mathcal{Z}_2(\mathcal{C})$ is the Müger center of \mathcal{C} . As special cases, this includes

$$\delta_{\text{modular}} = 0 \quad (81)$$

$$\delta_{\text{symmetric}} = \log \mathcal{D}^2 \quad (82)$$

We conjecture that Eq. (80) holds in generality. Physically, this is seen by noting that the particle content of the bulk Walker-Wang model is given by the Müger center $\mathcal{Z}_2(\cdot)$ [43].

Proof. Provided in Appendix B. □

Examples. Recall the examples from Section II A. As discussed in Section III C, these label four distinct loop-gas models in (3+1)-dimensions, the bosonic and fermionic toric code models, and two semion models. All four input categories are pointed, so we can apply Theorem 3 to obtain the TEE. The first two models are symmetric, so $\delta = \log 2$ for both. The inputs to the semion models are modular, so the bulk is trivial [27]. In this case $\delta = 0$.

VI. BOUNDARY ENTROPY OF TOPOLOGICAL LOOP-GASSES

We now turn to the computation of the boundary diagnostics from Section IV. As before, we begin with Levin-Wen models.

A. Levin-Wen models

Theorem 4 (Topological entropy of (2+1)D Levin-Wen models at a boundary).

Consider the regions shown in Fig. 2b. The Levin-Wen model defined by unitary spherical fusion category \mathcal{C} , with boundary specified by an indecomposable, strongly separable, special, Frobenius algebra $A \in \mathcal{C}$ has boundary entropy

$$\Gamma = \log \mathcal{D}^2, \quad (83)$$

where \mathcal{D} is the total quantum dimension of \mathcal{C} .

Examples. Recall the examples from Section II A. As discussed in Section III C, these label two distinct loop-gas models in (2+1)-dimensions, the toric code, and the double semion. The toric code has two possible boundary conditions, while the double semion only allows for the trivial boundary. All boundaries have $\Gamma = \log 2$.

Recall that a boundary for a Levin-Wen model defined by \mathcal{C} is specified by an algebra object $A \in \mathcal{C}$. The algebra encodes the strings that can terminate on the boundary. This interpretation leads us to the following lemma.

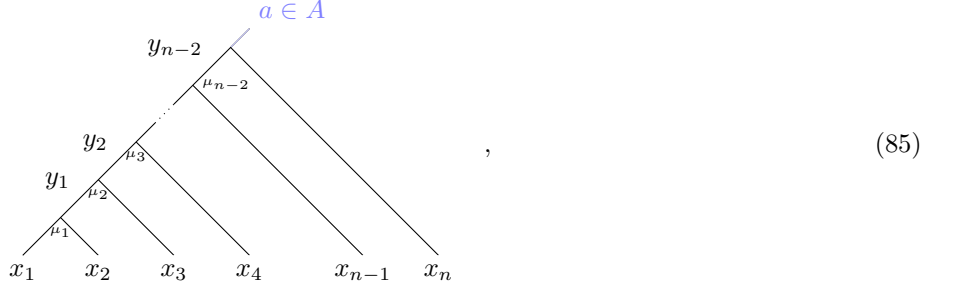
Lemma 8 (Entropy of (union of) simply connected regions, with boundary). *On a region R consisting of the disjoint union of simply connected sub-regions, the entropy is*

$$S_R = nS[\mathcal{C}] + \frac{b_1}{2} \log d_A - b_0 \log \mathcal{D}^2, \quad (84)$$

where b_0 is the number of disjoint interface components of R , b_1 is the number of points where the entanglement surface intersects the physical boundary, and n is the number of links crossing the entanglement interface.

Proof. Consider a ball R with n sites along the interface, which is in contact with the boundary. Recall that in the bulk, the fusion of the strings crossing the boundary was required to be 1. In the presence of the boundary, this

conservation rule is modified, since loops can terminate. All that is now required is that the fusion is in A



The ground state can be decomposed as

$$|\psi\rangle = \sum_{\substack{\vec{x}, \vec{y}, \vec{\mu} \\ a \in A}} \Phi_{\vec{x}, \vec{y}, \vec{\mu}, a} |\psi_R^{\vec{x}, \vec{y}, \vec{\mu}, a}\rangle |\psi_{R^c}^{\vec{x}, \vec{y}, \vec{\mu}, a}\rangle. \quad (86)$$

As before, the state $|\psi_R^{\vec{x}, \vec{y}, \vec{\mu}, a}\rangle$ includes any state that can be reached from Eq. (85) by acting only on R . The reduced state on R is

$$\rho_R = \sum_{\substack{\vec{x}, \vec{y}, \vec{\mu} \\ a \in A}} |\Phi_{\vec{x}, \vec{y}, \vec{\mu}, a}|^2 |\psi_R^{\vec{x}, \vec{y}, \vec{\mu}, a}\rangle \langle \psi_R^{\vec{x}, \vec{y}, \vec{\mu}, a}| \quad (87)$$

$$= \sum_{\substack{\vec{x}, \vec{y}, \vec{\mu} \\ a \in A}} \Pr[\vec{x}, \vec{y}, \vec{\mu} | a] \Pr[a] |\psi_R^{\vec{x}, \vec{y}, \vec{\mu}, a}\rangle \langle \psi_R^{\vec{x}, \vec{y}, \vec{\mu}, a}|, \quad (88)$$

where $\Pr[\vec{x}, \vec{y}, \vec{\mu} | a]$ is the probability of the labeled tree, given that \vec{x} fuses to a , and $\Pr[a \in A] = d_a/d_A$. Therefore,

$$\rho_R = \sum_{\substack{\vec{x}, \vec{y}, \vec{\mu} \\ a \in A}} \frac{\prod_{j \leq n} d_{x_j}}{\mathcal{D}^{2(n-1)} d_A} |\psi_R^{\vec{x}, \vec{y}, \vec{\mu}, a}\rangle \langle \psi_R^{\vec{x}, \vec{y}, \vec{\mu}, a}|. \quad (89)$$

Applying Lemmas 4 and 5 completes the proof for this region. It is straightforward to check that this holds on each sub-region of R , where Lemma 7 is used for any bulk sub-region. \square

Applying Lemma 8 to the regions in Fig. 2b completes the proof of Theorem 4.

We can make sense of this halving of the entropy by considering folding the plane. Suppose we fold the model in Fig. 2a so that it resembles Fig. 2b. This turns the bulk of a model defined by \mathcal{C} to a boundary of a model labeled by $\mathcal{C} \boxtimes \mathcal{C}^{\text{op}}$. The quantum dimension of the folded theory is $\mathcal{D}_{\mathcal{C} \boxtimes \mathcal{C}^{\text{op}}} = \mathcal{D}_{\mathcal{C}}^2$, so the bulk diagnostic for \mathcal{C} matches the boundary diagnostic computed for this folded theory.

B. Walker-Wang models

In 3D, just like in 2D, strings can terminate at the boundary. In addition, loops can interlock as discussed in Section V B. In the vicinity of the boundary, these two effects can occur simultaneously as depicted in Fig. 7.

For simply connected regions in contact with a boundary, we can apply Lemma 8, replacing $b_1/2$ with the number of lines where the region contacts the physical boundary. By applying the results so far, it is straightforward to check that the two diagnostics Eq. (49) and Eq. (50) are related by

$$\Delta_{\circ} = \Delta_{\bullet} + \log d_A^2 - \log \mathcal{D}^2, \quad (90)$$

so we only need to consider Δ_{\bullet} . We are currently unable to compute this in general, however in this section we prove the following results:

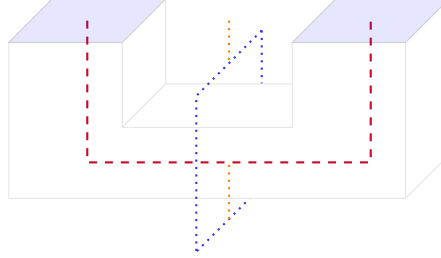


Figure 7: When the region R is in non-simple contact with a boundary on which strings can terminate, the computation of entropy is more subtle. There is additional entanglement in the system due to intersecting loops that cannot be created in R (red, dashed) or R^c (blue, dotted) separately. The red (internal) strings can terminate on the boundary. Also, the blue loop can emit a string which can terminate on the boundary.

Theorem 5. For a Walker-Wang model defined by a unitary premodular category \mathcal{C} , the entropy diagnostic Δ_\bullet for a boundary labeled by an indecomposable, strongly separable, commutative, Frobenius algebra A is given by

$$\Delta_\bullet = \begin{cases} \log \mathcal{D}^2 & A = 1, \\ \log \mathcal{D}^2 - \log d_A & \mathcal{C} \text{ symmetric,} \\ \log \mathcal{D}^2 - 2 \log d_A & \mathcal{C} \text{ pointed and } \mathcal{Z}_2(\mathcal{C}) \cap A = \{1\}. \text{ In particular } \mathcal{C} \text{ modular.} \\ \log \mathcal{D}^2 - \log d_A & \mathcal{C} \text{ pointed and } \mathcal{Z}_2(\mathcal{C}) \cap A = A. \end{cases} \quad (91)$$

Examples. Recall the examples from Section II A. As discussed in Section III C, these label four distinct loop-gas models in (3+1)-dimensions, the bosonic and fermionic toric code models, and two semion models. All four input categories are pointed, so we can apply Theorem 5 to obtain the boundary TEE.

The bosonic toric code is compatible with two distinct gapped boundary conditions, labeled by A_0 and A_1 (see Section II A), with $d_{A_0} = d_1 = 1$, and $d_{A_1} = d_1 + d_x = 2$. Since the input category is symmetric, $\mathcal{Z}_2(\mathcal{C}) \cap A_i = A_i$, so the entropy diagnostics are $\Delta_\bullet(A_0) = \log 2 - \log 1 = \log 2$ and $\Delta_\bullet(A_1) = \log 2 - \log 2 = 0$.

For the remaining examples, only the boundary labeled by A_0 is compatible, and $\Delta_\bullet = \log 2$ in all cases.

Proof. To capture configurations like the one in Fig. 7, we need new, boundary \mathcal{S} -matrices resembling

$$\frac{1}{\mathcal{D}} b_1 \begin{array}{c} \text{---} \\ \text{---} \\ \text{---} \\ \text{---} \\ \text{---} \end{array} \begin{array}{c} d \\ \text{---} \\ \text{---} \\ \text{---} \\ \text{---} \end{array} \begin{array}{c} a_1 \\ \text{---} \\ \text{---} \\ \text{---} \\ \text{---} \end{array} \begin{array}{c} b_0 \\ \text{---} \\ \text{---} \\ \text{---} \\ \text{---} \end{array} \begin{array}{c} \text{---} \\ \text{---} \\ \text{---} \\ \text{---} \\ \text{---} \end{array} \begin{array}{c} a_0 \\ \text{---} \\ \text{---} \\ \text{---} \\ \text{---} \end{array} , \quad (92)$$

where the dots indicate where a string meets the boundary. We use boundary retriangulation invariance, as defined in Refs. 11 and 12 to evaluate this diagram on the ground space. Using this, we define the new \mathcal{S} -matrix elements as

$$[\mathcal{S}_{c,d}]_{(b_0,b_1),(a_0,a_1)} := \frac{m_{a_1,a_0}^{\bar{d}}}{(d_{a_0} d_{a_1} d_{\bar{d}})^{1/4} d_A \mathcal{D}} b_1 \begin{array}{c} \text{---} \\ \text{---} \\ \text{---} \\ \text{---} \\ \text{---} \end{array} \begin{array}{c} d \\ \text{---} \\ \text{---} \\ \text{---} \\ \text{---} \end{array} \begin{array}{c} a_1 \\ \text{---} \\ \text{---} \\ \text{---} \\ \text{---} \end{array} \begin{array}{c} b_0 \\ \text{---} \\ \text{---} \\ \text{---} \\ \text{---} \end{array} \begin{array}{c} \text{---} \\ \text{---} \\ \text{---} \\ \text{---} \\ \text{---} \end{array} \begin{array}{c} a_0 \\ \text{---} \\ \text{---} \\ \text{---} \\ \text{---} \end{array} , \quad (93)$$

where $a_0, a_1, d \in A$ and $b_0, b_1, c \in \mathcal{C}$. With this, the ground state can be written

$$|\psi\rangle = \sum_{\substack{\vec{x}, \vec{y}, \vec{\mu} \\ c, b_0, b_1 \in \mathcal{C} \\ d, a_0, a_1 \in A}} \Phi_{\vec{x}, \vec{y}, \vec{\mu}, c} \frac{[\mathcal{S}_{c,d}]_{(b_0,b_1),(a_0,a_1)}}{N_A} \left| \psi_R^{\vec{x}, \vec{y}, \vec{\mu}, c, a_0, a_1} \right\rangle \left| \psi_{R^c}^{\vec{x}, \vec{y}, \vec{\mu}, c, b_0, b_1, d} \right\rangle , \quad (94)$$

where N_A is a normalizing factor. The reduced state on R is

$$\rho_R = \sum_{\substack{\vec{x}, \vec{y}, \vec{\mu} \\ c \in \mathcal{C} \\ d, a_0, a_1, a_2, a_3 \in A}} \frac{\prod_{j \leq n} d_{x_j} [\mathcal{S}_{c,d}^\dagger \mathcal{S}_{c,d}]_{(a_2, a_3), (a_0, a_1)}}{d_c \mathcal{D}^{2(n-1)} N_A} \left| \psi_R^{\vec{x}, \vec{y}, \vec{\mu}, c, a_0, a_1} \right\rangle \left\langle \psi_R^{\vec{x}, \vec{y}, \vec{\mu}, c, a_2, a_3} \right|. \quad (95)$$

1. $A = 1$

When the algebra is trivial, no strings can terminate. In that case, $\mathcal{S}_{1,1}^\dagger \mathcal{S}_{1,1} = 1$, so the reduced state is

$$\rho_R = \sum_{\vec{x}, \vec{y}, \vec{\mu}} \frac{\prod_{j \leq n} d_{x_j}}{\mathcal{D}^{2(n-1)}} \left| \psi_R^{\vec{x}, \vec{y}, \vec{\mu}} \right\rangle \left\langle \psi_R^{\vec{x}, \vec{y}, \vec{\mu}} \right|, \quad (96)$$

which is diagonal and has entropy

$$S_R = nS[C] - \log \mathcal{D}^2. \quad (97)$$

2. \mathcal{C} symmetric

When \mathcal{C} is symmetric, the rings in Eq. (93) separate, so

$$[\mathcal{S}_{c,d}]_{(b_0, b_1), (a_0, a_1)} = \delta_{c=d} \sqrt{d_{b_0} d_{b_1}} \frac{(d_{a_0} d_{a_1})^{1/4} m_{a_1, a_0}^{\bar{d}}}{d_d^{1/4} d_A^2 \mathcal{D}}, \quad (98)$$

$$[\mathcal{S}_{c,d}^\dagger \mathcal{S}_{c,d}]_{(a_2, a_3), (a_0, a_1)} = \delta_{c=d} \sum_{b_0, b_1} N_{b_0 b_1}^d \frac{d_{b_0} d_{b_1}}{\sqrt{d_d}} (d_{a_0} d_{a_1} d_{a_2} d_{a_3})^{1/4} \frac{m_{a_1, a_0}^{\bar{d}} \left(m_{a_3, a_2}^{\bar{d}} \right)^*}{d_A^4 \mathcal{D}^2} \quad (99)$$

$$= \delta_{c=d} (d_{a_0} d_{a_1} d_{a_2} d_{a_3})^{1/4} \sqrt{d_d} \frac{m_{a_1, a_0}^{\bar{d}} \left(m_{a_3, a_2}^{\bar{d}} \right)^*}{d_A^2}. \quad (100)$$

It can readily be verified that this matrix is rank 1. The eigenvalue can be found using Eq. (36), giving $\lambda = d_d/d_A$. We can therefore write the state on R as

$$\rho_R = \sum_{\substack{\vec{x}, \vec{y}, \vec{\mu} \\ c \in \mathcal{C} \\ d \in A}} \delta_{c=d} \frac{\prod_{j \leq n} d_{x_j}}{\mathcal{D}^{2(n-1)} d_A} \left| \psi_R^{\vec{x}, \vec{y}, \vec{\mu}, c} \right\rangle \left\langle \psi_R^{\vec{x}, \vec{y}, \vec{\mu}, c} \right| \quad (101)$$

$$= \sum_{\substack{\vec{x}, \vec{y}, \vec{\mu} \\ c \in A}} \frac{\prod_{j \leq n} d_{x_j}}{\mathcal{D}^{2(n-1)} d_A} \left| \psi_R^{\vec{x}, \vec{y}, \vec{\mu}, c} \right\rangle \left\langle \psi_R^{\vec{x}, \vec{y}, \vec{\mu}, c} \right|. \quad (102)$$

Using Lemmas 4 and 5, entropy of this state is

$$S_R = nS[\mathcal{C}] - \log \mathcal{D}^2 + \log d_A. \quad (103)$$

3. \mathcal{C} pointed

When all quantum dimensions are equal to 1, the boundary \mathcal{S} -matrix is

$$[\mathcal{S}_{c,d}]_{(b_0, b_1), (a_0, a_1)} = \delta_{c=d} \frac{m_{a_1, a_0}^{\bar{d}}}{d_A} [\mathcal{S}]_{b_0, \bar{a}_1}, \quad (104)$$

where $[\mathcal{S}]_{b_0, a_1}$ is the \mathcal{S} -matrix from Eq. (15). This gives

$$[\mathcal{S}_{c,d}^\dagger \mathcal{S}_{c,d}]_{(a_2, a_3), (a_0, a_1)} = \delta_{c=d} \frac{m_{a_1, a_0}^{\bar{d}} (m_{a_3, a_2}^{\bar{d}})^*}{d_A^2} \sum_{b_0} [\mathcal{S}]_{b_0, \bar{a}_3}^* [\mathcal{S}]_{b_0, \bar{a}_1}. \quad (105)$$

Using Lemmas 1 and 2, this can be simplified to

$$[\mathcal{S}_{c,d}^\dagger \mathcal{S}_{c,d}]_{(a_2, a_3), (a_0, a_1)} = \delta_{c=d} \frac{m_{a_1, a_0}^{\bar{d}} (m_{a_3, a_2}^{\bar{d}})^*}{d_A^2} \delta_{a_3 \otimes \bar{a}_1 \in \mathcal{Z}_2(\mathcal{C})}. \quad (106)$$

Pointed braided categories have fusion rules given by an Abelian group G [33, 59], and algebras are twisted group algebras [60, 61] of subgroups of G . Moreover, $\mathcal{Z}_2(\mathcal{C})$ also has fusion rules given by a subgroup G .

Since $a_3 \otimes \bar{a}_1 \in A$ and $a_3 \otimes \bar{a}_1 \in \mathcal{Z}_2(\mathcal{C})$, there must be some $h \in \mathcal{Z}_2(\mathcal{C}) \cap A$ so that $a_3 = a_1 h$. We can then write

$$\rho_R = \sum_{\substack{\vec{x} \\ d, a \in A \\ h \in \mathcal{Z}_2(\mathcal{C}) \cap A}} \frac{m_{a, (ad)^{-1}}^{d^{-1}} (m_{ah, (ahd)^{-1}}^{d^{-1}})^*}{d_A^2 \mathcal{D}^{2(n-1)} N_A} \left| \psi_R^{\vec{x}, d, a} \right\rangle \left\langle \psi_R^{\vec{x}, d, ah} \right|. \quad (107)$$

In the case that $\mathcal{Z}_2(\mathcal{C}) \cap A = A$, this reduces to the symmetric case, since summing over $h \in A$ is the same as summing over $A \ni h' = ah$.

When $\mathcal{Z}_2(\mathcal{C}) \cap A = \{1\}$, the state on R simplifies to

$$\rho_R = \sum_{\substack{\vec{x} \\ d, a \in A}} \frac{m_{a, (ad)^{-1}}^{d^{-1}} (m_{a, (ad)^{-1}}^{d^{-1}})^*}{d_A^2 \mathcal{D}^{2(n-1)} N_A} \left| \psi_R^{\vec{x}, d, a} \right\rangle \left\langle \psi_R^{\vec{x}, d, a} \right|. \quad (108)$$

This state is diagonal, and has entropy

$$S_R = - \sum_{\substack{\vec{x} \\ d, a \in A}} \frac{|m_{a, (ad)^{-1}}^{d^{-1}}|^2}{\mathcal{D}^{2(n-1)} d_A^2} \log \left(\frac{|m_{a, (ad)^{-1}}^{d^{-1}}|^2}{\mathcal{D}^{2(n-1)} d_A^2} \right) \quad (109)$$

$$= - \sum_{\substack{\vec{x} \\ d, a \in A}} \frac{|m_{a, (ad)^{-1}}^{d^{-1}}|^2}{\mathcal{D}^{2(n-1)} d_A^2} \log \left(|m_{a, (ad)^{-1}}^{d^{-1}}|^2 \right) + \log \left(\mathcal{D}^{2(n-1)} d_A^2 \right), \quad (110)$$

where we have made use of Eq. (36). Since A is a twisted group algebra, we may assume $|m_{ab}^c| \in \{0, 1\}$. Finally, this gives

$$S_R = \log \left(\mathcal{D}^{2(n-1)} d_A^2 \right) \quad (111)$$

$$= S[\mathcal{C}] - \log \mathcal{D}^2 + 2 \log d_A, \quad (112)$$

completing the proof. \square

VII. REMARKS

To summarize, we have evaluated the long-range entanglement in the bulk, and at the boundary, of (2+1)- and (3+1)-dimensional topological phases. In (2+1) dimensions, we found the entropy diagnostic $\Gamma = \log \mathcal{D}^2$ regardless of the choice of boundary algebra A . This is in contrast to the results for three dimensions, where a signature of the boundary, namely its dimension as an algebra, can be seen in the diagnostics Δ_\bullet and Δ_\circ .

The most natural boundary for these models is defined by the algebra $A = 1$, which (uniquely) always exists. At this boundary, we found that the point-like diagnostic Δ_\bullet recovers the total dimension of the input category. In particular, when \mathcal{C} is a (2+1)D anyon model, this is consistent with a boundary that supports the anyons. Conversely, the loop-like

diagnostic Δ_0 is zero at these boundaries, ruling out loop-like excitations in the vicinity.

We have conjectured a general property of the connected \mathcal{S} -matrix which, if proven in general, allows computation of bulk WW topological entropy. Such a proof may also be interesting for the classification of premodular categories in general. To the best of our knowledge, there is no complete classification of boundaries for Walker-Wang models. Such a classification is complicated by requiring, as a sub-classification, a complete understanding of (2+1)D theories. This goes beyond the scope of the current work, and we have therefore specialized to boundaries described by Frobenius algebras and to particular families of input fusion category. Extending these results may provide a more complete understanding of the possible boundary excitations and their properties.

ACKNOWLEDGMENTS

We particularly thank David Aasen for useful discussions, and informing us of the class of Walker-Wang boundaries we consider. We are also grateful to Taiga Adair, Daniel Barter, Isaac Kim, Sam Roberts, Thomas Smith and Dominic Williamson for helpful discussions. We also thank Stephen Bartlett and Céline Boehm.

Research at Perimeter Institute is supported in part by the Government of Canada through the Department of Innovation, Science and Industry Canada and by the Province of Ontario through the Ministry of Colleges and Universities. This work is supported by the Australian Research Council (ARC) via the Centre of Excellence in Engineered Quantum Systems (EQuS) project number CE170100009. BJB was previously supported by the University of Sydney Fellowship Programme. SJE also received support from the EPSRC.

[1] F. D. M. Haldane and E. H. Rezayi, Periodic Laughlin-Jastrow wave functions for the fractional quantized Hall effect, *Phys. Rev. B* **31**, 2529 (1985).

[2] X. G. Wen, Vacuum degeneracy of chiral spin states in compactified space, *Phys. Rev. B* **40**, 7387 (1989).

[3] X. G. Wen and Q. Niu, Ground-state degeneracy of the fractional quantum Hall states in the presence of a random potential and on high-genus Riemann surfaces, *Phys. Rev. B* **41**, 9377 (1990).

[4] X.-G. Wen, *Quantum field theory of many-body systems: from the origin of sound to an origin of light and electrons* (Oxford University Pres, 2004).

[5] A. Y. Kitaev, Fault-tolerant quantum computation by anyons, *Ann. Phys.* **303**, 2, arXiv:quant-ph/9707021 (2003).

[6] B. J. Brown, D. Loss, J. K. Pachos, C. N. Self, and J. R. Wootton, Quantum memories at finite temperature, *Rev. Mod. Phys.* **88**, 045005, arXiv:1411.6643 (2016).

[7] F. Wilczek, Magnetic flux, angular momentum, and statistics, *Phys. Rev. Lett.* **48**, 1144 (1982).

[8] F. Wilczek, Quantum mechanics of fractional-spin particles, *Phys. Rev. Lett.* **49**, 957 (1982).

[9] M. A. Levin and X.-G. Wen, String-net condensation: A physical mechanism for topological phases, *Phys. Rev. B* **71**, 045110, arXiv:cond-mat/0404617 (2005).

[10] K. Walker and Z. Wang, (3+1)-TQFTs and topological insulators, *Front. Phys.* **7**, 150, arXiv:1104.2632 (2012).

[11] Y. Hu, Z.-X. Luo, R. Pankovich, Y. Wan, and Y.-S. Wu, Boundary Hamiltonian theory for gapped topological phases on an open surface, *J. High Energy Phys.* **2018**, 134, arXiv:1706.03329 (2018).

[12] Y. Hu, Y. Wan, and Y.-S. Wu, Boundary Hamiltonian theory for gapped topological orders, *Chin. Phys. Lett.* **34**, 077103, arXiv:1706.00650 (2017).

[13] X. Chen, Z.-C. Gu, and X.-G. Wen, Local unitary transformation, long-range quantum entanglement, wave function renormalization, and topological order, *Phys. Rev. B* **82**, 155138, arXiv:1004.3835 (2010).

[14] Z. Wang and X. Chen, Twisted gauge theories in three-dimensional Walker-Wang models, *Phys. Rev. B* **95**, 115142, arXiv:1611.09334 (2017).

[15] A. Hamma, R. Ionicioiu, and P. Zanardi, Bipartite entanglement and entropic boundary law in lattice spin systems, *Phys. Rev. A* **71**, 022315, arXiv:quant-ph/0409073 (2005).

[16] A. Kitaev and J. Preskill, Topological entanglement entropy, *Phys. Rev. Lett.* **96**, 110404, arXiv:hep-th/0510092 (2006).

[17] M. Levin and X.-G. Wen, Detecting topological order in a ground state wave function, *Phys. Rev. Lett.* **96**, 110405, arXiv:cond-mat/0510613 (2006).

[18] J. Eisert, M. Cramer, and M. B. Plenio, Colloquium: Area laws for the entanglement entropy, *Rev. Mod. Phys.* **82**, 277, arXiv:0808.3773 (2010).

[19] S. Dong, E. Fradkin, R. G. Leigh, and S. Nowling, Topological entanglement entropy in Chern-Simons theories and quantum Hall fluids, *J. High Energy Phys.* **2008**, 016, arXiv:0802.3231 (2008).

[20] B. J. Brown, S. D. Bartlett, A. C. Doherty, and S. D. Barrett, Topological entanglement entropy with a twist, *Phys. Rev. Lett.* **111**, 220402, arXiv:1303.4455 (2013).

[21] P. Bonderson, C. Knapp, and K. Patel, Anyonic entanglement and topological entanglement entropy, *Ann. Phys.* **385**, 399, arXiv:1706.09420 (2017).

- [22] B. Shi, K. Kato, and I. H. Kim, Fusion rules from entanglement, *Annals of Physics* **418**, 168164, arXiv:1906.09376 (2020).
- [23] Y. Zhang, T. Grover, A. Turner, M. Oshikawa, and A. Vishwanath, Quasiparticle statistics and braiding from ground-state entanglement, *Phys. Rev. B* **85**, 235151, arXiv:1111.2342 (2012).
- [24] C. Castelnovo and C. Chamon, Topological order in a three-dimensional toric code at finite temperature, *Phys. Rev. B* **78**, 155120, arXiv:0804.3591 (2008).
- [25] T. Grover, A. M. Turner, and A. Vishwanath, Entanglement entropy of gapped phases and topological order in three dimensions, *Phys. Rev. B* **84**, 195120, arXiv:1108.4038 (2011).
- [26] A. Hamma, P. Zanardi, and X.-G. Wen, String and membrane condensation on three-dimensional lattices, *Phys. Rev. B* **72**, 035307, arXiv:cond-mat/0411752 (2005).
- [27] C. W. von Keyserlingk, F. J. Burnell, and S. H. Simon, Three-dimensional topological lattice models with surface anyons, *Phys. Rev. B* **87**, 045107, arXiv:1208.5128 (2013).
- [28] A. Bullivant and J. K. Pachos, Entropic manifestations of topological order in three dimensions, *Phys. Rev. B* **93**, 125111, arXiv:1504.02868 (2016).
- [29] I. H. Kim and B. J. Brown, Ground-state entanglement constrains low-energy excitations, *Phys. Rev. B* **92**, 115139, arXiv:1410.7411 (2015).
- [30] B. Shi and Y.-M. Lu, Characterizing topological order by the information convex, *Phys. Rev. B* **99**, 035112, arXiv:1801.01519 (2019).
- [31] M. Müger, From Subfactors to Categories and Topology I. Frobenius algebras in and Morita equivalence of tensor categories, *J. Pure Appl. Algebra* **180**, 81, arXiv:math/0111204 (2003).
- [32] M. Müger, Tensor categories: A selective guided tour, *Rev. de la Union Mat. Argentina* **51**, 95, arXiv:0804.3587 (2010).
- [33] P. Etingof, S. Gelaki, D. Nikshych, and V. Ostrik, *Tensor categories*, Mathematical Surveys and Monographs, Vol. 205 (American Mathematical Society, Providence, RI, 2015) pp. xvi+343.
- [34] A. Kitaev, Anyons in an exactly solved model and beyond, *Ann. Phys.* **321**, 2, arXiv:cond-mat/0506438 (2006).
- [35] P. H. Bonderson, *Non-Abelian Anyons and Interferometry*, Ph.D. thesis, California Institute of Technology (2007).
- [36] We refrain from drawing arrows on the diagrams, instead using the convention that all lines are oriented upwards.
- [37] P. Bonderson, C. Delaney, C. Galindo, E. C. Rowell, A. Tran, and Z. Wang, On invariants of modular categories beyond modular data, *Journal of Pure and Applied Algebra* **223**, 4065, arXiv:1805.05736 (2019).
- [38] J. C. Bridgeman, *UnitaryPremodularCategoryData*, github.com/JCBridgeman/UnitaryPremodularCategoryData, Github repository (2020).
- [39] The lattice is the dual of the triangulation.
- [40] D. J. Williamson and Z. Wang, Hamiltonian models for topological phases of matter in three spatial dimensions, *Ann. Phys.* **377**, 311, arXiv:1606.07144 (2017).
- [41] L. Crane and D. Yetter, A categorical construction of 4D topological quantum field theories, *Quant. Topol.* **3**, 120, arXiv:hep-th/9301062 (1993).
- [42] L. Crane, L. H. Kauffman, and D. N. Yetter, State-sum invariants of 4-manifolds, *J. Knot Theory Ramif.* **6**, 177, arXiv:hep-th/9409167 (1997).
- [43] Z. Wang, *Topological Phases of Matter: Exactly Solvable Models and Classification*, Ph.D. thesis, California Institute of Technology (2019).
- [44] J. Fuchs, I. Runkel, and C. Schweigert, TFT construction of RCFT correlators I: partition functions, *Nucl. Phys. B* **646**, 353, arXiv:hep-th/0204148 (2002).
- [45] A. Y. Kitaev and L. Kong, Models for gapped boundaries and domain walls, *Commun. Math. Phys.* **313**, 351, arXiv:1104.5047 (2012).
- [46] J. Fuchs, C. Schweigert, and A. Valentino, Bicategories for boundary conditions and for surface defects in 3-D TFT, *Commun. Math. Phys.* **321**, 543, arXiv:1203.4568 (2013).
- [47] J. Fuchs, J. Priel, C. Schweigert, and A. Valentino, On the Brauer groups of symmetries of abelian Dijkgraaf-Witten theories, *Commun. Math. Phys.* **339**, 385, arXiv:1404.6646 (2015).
- [48] Private communications with David Aasen.
- [49] S. B. Bravyi and A. Y. Kitaev, Quantum codes on a lattice with boundary, arXiv:quant-ph/9811052 (1998).
- [50] C. W. von Keyserlingk and F. J. Burnell, Walker-Wang models and axion electrodynamics, *Phys. Rev. B* **91**, 045134, arXiv:1405.2988 (2015).
- [51] S. Bravyi, Unpublished.
- [52] J. Cano, T. L. Hughes, and M. Mulligan, Interactions along an entanglement cut in 2 + 1d Abelian topological phases, *Phys. Rev. B* **92**, 075104, arXiv:1411.5369 (2015).
- [53] L. Zou and J. Haah, Spurious long-range entanglement and replica correlation length, *Phys. Rev. B* **94**, 075151, arXiv:1604.06101 (2016).
- [54] D. J. Williamson, A. Dua, and M. Cheng, Spurious topological entanglement entropy from subsystem symmetries, *Phys. Rev. Lett.* **122**, 140506, arXiv:1808.05221 (2019).
- [55] K. Kato and F. G. Brandão, Toy model of boundary states with spurious topological entanglement entropy, *Phys. Rev. Research* **2**, 032005(R), arXiv:1911.09819 (2020).
- [56] M. Levin, *String-net condensation and topological phases in quantum spin systems*, Ph.D. thesis, Massachusetts Institute of Technology (2006).
- [57] D. Tambara and S. Yamagami, Tensor categories with fusion rules of self-duality for finite abelian groups, *Journal of*

Algebra **209**, 692 (1998).

[58] J. A. Siehler, Braided near-group categories, [arXiv:math/0011037](https://arxiv.org/abs/math/0011037) (2000).

[59] A. Joyal and R. Street, Braided tensor categories, *Adv. Math.* **102**, 20 (1993).

[60] V. Ostrik, Module categories over the Drinfeld double of a finite group, *Int. Math. Res. Not.* **2003**, 1507, [arXiv:math/0202130](https://arxiv.org/abs/math/0202130) (2003).

[61] A. Bullivant and C. Delcamp, Gapped boundaries and string-like excitations in (3+1)d gauge models of topological phases, [arXiv:2006.06536](https://arxiv.org/abs/2006.06536) (2020).

[62] J. Preskill, *Lecture notes for physics 219: Quantum computation*, chapter 9 (2004).

[63] V. Ostrik, Fusion categories of rank 2, *Math. Res. Lett.* **10**, 177, [arXiv:math/0203255](https://arxiv.org/abs/math/0203255) (2003).

[64] V. Ostrik, Pre-modular categories of rank 3, *Mosc. Math. J.* **8**, 111, [arXiv:math/0503564](https://arxiv.org/abs/math/0503564) (2008).

[65] E. Rowell, R. Stong, and Z. Wang, On classification of modular tensor categories, *Commun. Math. Phys.* **292**, 343, [arXiv:0712.1377](https://arxiv.org/abs/0712.1377) (2009).

[66] P. Bruillard, Rank 4 premodular categories, *New York J. Math.* **22**, 775, [arXiv:1204.4836](https://arxiv.org/abs/1204.4836) (2016).

[67] P. Bruillard and C. M. Ortiz-Marrero, Classification of rank 5 premodular categories, *J. Math. Phys.* **59**, 011702, [arXiv:1612.08769](https://arxiv.org/abs/1612.08769) (2018).

[68] Z. Yu, On slightly degenerate fusion categories, *J. Algebra* **559**, 408, [arXiv:1903.06345](https://arxiv.org/abs/1903.06345) (2020).

[69] [List of small multiplicity-free fusion rings](#), accessed November 1 2020.

Lemma 1. Let \mathcal{C} be a unitary premodular category. The matrix elements of \mathcal{S} obey

$$\frac{\mathcal{D}}{d_c} \mathcal{S}_{a,c} \mathcal{S}_{b,c} = \mathcal{S}_{a \otimes b, c} = \sum_x N_{a,b}^x \mathcal{S}_{x,c}. \quad (\text{A1})$$

Proof. We prove the second equality first.

$$\mathcal{S}_{a \otimes b, c} := \frac{1}{\mathcal{D}} \bar{b} \left(\begin{array}{c} \text{circle} \\ \text{circle} \end{array} \right) \left(\begin{array}{c} \text{circle} \\ \text{circle} \end{array} \right) c = \frac{1}{\mathcal{D}} \sum_x \sum_{\mu=1}^{N_{a,b}^x} \sqrt{\frac{d_x}{d_a d_b}} \bar{b} \left(\begin{array}{c} \text{circle} \\ \text{circle} \end{array} \right) \left(\begin{array}{c} \text{circle} \\ \text{circle} \end{array} \right) c \quad (\text{A2})$$

$$= \frac{1}{\mathcal{D}} \sum_{x,\mu} \sqrt{\frac{d_x}{d_a d_b}} \bar{b} \left(\begin{array}{c} \text{circle} \\ \text{circle} \end{array} \right) \left(\begin{array}{c} \text{circle} \\ \text{circle} \end{array} \right) c = \sum_x N_{a,b}^x \mathcal{S}_{x,c}. \quad (\text{A3})$$

And the first equality.

$$\frac{1}{\mathcal{D}} \bar{b} \left(\begin{array}{c} \text{circle} \\ \text{circle} \end{array} \right) \left(\begin{array}{c} \text{circle} \\ \text{circle} \end{array} \right) c = \frac{1}{\mathcal{D}} \sum_{x,\mu} \sqrt{\frac{d_x}{d_a d_c}} \frac{\theta_x}{\theta_a \theta_{\bar{c}}} \left(\begin{array}{c} \text{circle} \\ \text{circle} \end{array} \right) \left(\begin{array}{c} \text{circle} \\ \text{circle} \end{array} \right) c = \frac{1}{\mathcal{D}} \sum_{x,\mu} \sqrt{\frac{d_x}{d_a d_c}} \frac{\theta_x}{\theta_a \theta_{\bar{c}}} \left(\begin{array}{c} \text{circle} \\ \text{circle} \end{array} \right) \left(\begin{array}{c} \text{circle} \\ \text{circle} \end{array} \right) c \quad (\text{A4})$$

$$= \left(\frac{1}{\mathcal{D} d_c} \sum_x \frac{\theta_x}{\theta_a \theta_{\bar{c}}} d_x \right) \left(\begin{array}{c} \text{circle} \\ \text{circle} \end{array} \right) \left(\begin{array}{c} \text{circle} \\ \text{circle} \end{array} \right) c = \frac{\mathcal{S}_{a,c}}{d_c} \left(\begin{array}{c} \text{circle} \\ \text{circle} \end{array} \right) \left(\begin{array}{c} \text{circle} \\ \text{circle} \end{array} \right) c = \frac{\mathcal{D} \mathcal{S}_{a,c} \mathcal{S}_{b,c}}{d_c}. \quad (\text{A5})$$

□

Lemma 2. Let \mathcal{C} be a unitary premodular category, then

$$\sum_b d_b \mathcal{S}_{a,b} = \delta_{a \in \mathcal{Z}_2(\mathcal{C})} d_a \mathcal{D}, \quad (\text{A6})$$

where $\delta_W = 1 \iff W$ is true, and $\mathcal{Z}_2(\mathcal{C})$ is the Müger center.

Proof. If $a \in \mathcal{Z}_2(\mathcal{C})$, then

$$\sum_b d_b \mathcal{S}_{a,b} = \frac{1}{\mathcal{D}} \sum_{x,b} N_{a,\bar{b}}^x d_x d_b \quad (\text{A7})$$

$$= \frac{1}{\mathcal{D}} \sum_b d_a d_b^2 \quad (\text{A8})$$

$$= \mathcal{D} d_a \quad (\text{A9})$$

Otherwise, we have

$$\frac{\mathcal{D}}{d_a} \mathcal{S}_{a,c} \sum_b d_b \mathcal{S}_{a,b} = \sum_{x,b} N_{c,b}^x \mathcal{S}_{a,x} d_b = \sum_x \mathcal{S}_{a,x} d_x d_c, \quad (\text{A10})$$

so after relabeling the RHS summation variable

$$\sum_b d_b \mathcal{S}_{a,b} \left(\mathcal{S}_{a,c} - \frac{d_a d_c}{\mathcal{D}} \right) = 0, \quad (\text{A11})$$

for all c . Unless $\mathcal{C} = \mathcal{Z}_2(\mathcal{C})$ (in which case, $a \in \mathcal{Z}_2(\mathcal{C})$), this implies the result. □

Lemma 3. Let \mathcal{C} be a unitary premodular category, then

$$\sum_{c \in \mathcal{C}} \text{Tr } \mathcal{S}_c^\dagger \mathcal{S}_c = \mathcal{D}^2, \quad (\text{A12})$$

where \mathcal{S}_c is the connected \mathcal{S} -matrix and \mathcal{D} is the total dimension of \mathcal{C} .

Proof. Using Eq. (19), we have

$$\sum_c \text{Tr } \mathcal{S}_c^\dagger \mathcal{S}_c = \sum_{a, \alpha, c} [\mathcal{S}_c^\dagger \mathcal{S}_c]_{(a, \alpha), (a, \alpha)} \quad (\text{A13})$$

$$= \sum_{a, \alpha, c} \frac{\sqrt{d_c}}{\mathcal{D}^2} \sum_x d_x \quad \text{Diagram: } \begin{array}{c} c \\ \alpha \\ \bar{a} \end{array} \text{ (left)} \quad \begin{array}{c} \text{Diagram: } \text{Three circles } a, x, \bar{a} \text{ connected by arcs. } \\ \text{Top arc: } c \rightarrow a \\ \text{Middle arc: } \alpha \rightarrow x \\ \text{Bottom arc: } \bar{a} \rightarrow \bar{c} \end{array} \quad \text{Diagram: } \begin{array}{c} \bar{a} \\ \alpha \\ x \\ a \\ \alpha \\ c \\ \bar{a} \end{array} \quad (\text{A14})$$

$$= \sum_{a, \alpha, c} \frac{\sqrt{d_c}}{\mathcal{D}^2} \sum_x d_x \quad \text{Diagram: } \begin{array}{c} \bar{a} \\ \alpha \\ x \\ a \\ \alpha \\ c \\ \bar{a} \end{array} \quad (\text{A15})$$

using the properties of the trace. Applying the premodular trap (Corollary 1), this gives

$$\sum_c \text{Tr } \mathcal{S}_c^\dagger \mathcal{S}_c = \sum_{\substack{a, \alpha, c, \\ z \in \mathcal{Z}_2(\mathcal{C}), \mu}} \sqrt{\frac{d_c d_z}{d_a^2}} \quad \text{Diagram: } \begin{array}{c} \mu \\ z \\ \bar{a} \\ \mu \\ \alpha \\ a \\ \bar{a} \\ c \\ \alpha \\ a \end{array} \quad (\text{A16})$$

$$= \sum_{a, z \in \mathcal{Z}_2(\mathcal{C}), \mu} \sqrt{d_z} \quad \text{Diagram: } \begin{array}{c} \mu \\ z \\ \mu \end{array} \quad (\text{A17})$$

$$= \sum_{a, z \in \mathcal{Z}_2(\mathcal{C}), \mu} |\kappa_a|^2 \delta_{z=1} d_a^2 \quad (\text{A18})$$

$$= \mathcal{D}^2, \quad (\text{A19})$$

where κ_a is the Frobenius-Schur indicator [34]. \square

In this section, given a fusion category \mathcal{C} , an n -tuple of simple objects $\vec{x}_n := (x_1, x_2, \dots, x_n)$, and a fixed simple object a , we use the notation

$$N_a(\vec{x}_n) := \sum_{\vec{y}_{n-2}} N_{x_1, x_2}^{y_1} N_{y_1, x_3}^{y_2} \dots N_{y_{n-2}, x_n}^a, \quad (\text{B1})$$

where $\vec{y}_{n-2} := (y_1, y_2, \dots, y_{n-2})$, and the sum is over all tuples of simple objects in \mathcal{C} . $N_a(\vec{x}_n)$ counts the number of ways \vec{x}_n can fuse to a . When it can easily be inferred, we omit the subscript on the tuple \vec{x} .

Lemma 4. *Let \mathcal{C} a unitary fusion category, then*

$$\sum_{\vec{x}_n} N_a(\vec{x}_n) \prod_{j \leq n} d_{x_j} = d_a \mathcal{D}^{2(n-1)}, \quad (\text{B2})$$

where $\mathcal{D} = \sqrt{\sum_a d_a^2}$ is the total quantum dimension of \mathcal{C} .

Proof. We proceed inductively.

When $n = 1$, $N_a(x) = \delta_{x=a} = N_{1,x}^a$, and Eq. (B2) reduces to $d_a = d_a$.

Assume Eq. (B2) holds for the fusion of n objects. Recall that for any fusion category, we have

$$d_a d_b = \sum_c N_{bc}^a d_c, \quad (\text{B3})$$

and this holds for any cyclic permutation of the indices on N_{bc}^a . We now obtain

$$\sum_{\vec{x}_{n+1}} N_a(\vec{x}_{n+1}) \prod_{j \leq n+1} d_{x_j} = \sum_{\vec{x}_n, y_{n-1}} N_{y_{n-1}}(\vec{x}_n) \prod_{j \leq n} d_{x_j} \sum_{x_{n+1}} N_{y_{n-1}, x_{n+1}}^a d_{x_{n+1}} \quad (\text{B4})$$

$$= \mathcal{D}^{2(n-1)} \sum_{x_{n+1}, y_{n-1}} N_{y_{n-1}, x_{n+1}}^a d_{y_{n-1}} d_{x_{n+1}} \quad (\text{B5})$$

$$= \mathcal{D}^{2(n-1)} d_a \sum_{y_{n-1}} d_{y_{n-1}}^2 \quad (\text{B6})$$

$$= d_a \mathcal{D}^{2n}, \quad (\text{B7})$$

where in the second line we used the induction assumption (Eq. (B2)), and in the third line we used Eq. (B3). \square

Lemma 5. *Let \mathcal{C} a unitary fusion category. For the fusion of n objects $\vec{x} = (x_1, x_2, \dots, x_n)$, with $n > 1$, we have*

$$\sum_{\vec{x}_n} N_a(\vec{x}_n) \frac{\prod_{j \leq n} d_{x_j}}{\mathcal{D}^{2(n-1)}} \log \prod_{k \leq n} d_{x_k} = n d_a \sum_x \frac{d_x^2 \log d_x}{\mathcal{D}^2}. \quad (\text{B8})$$

Proof. We prove the claim inductively. The base case is when $n = 2$.

$$\sum_{x_1, x_2} N_{x_1, x_2}^a \frac{d_{x_1} d_{x_2}}{\mathcal{D}^2} (\log d_{x_1} + \log d_{x_2}) = \sum_{x_1, x_2} N_{x_1, x_2}^a \frac{d_{x_1} d_{x_2}}{\mathcal{D}^2} \log d_{x_1} + \sum_{x_1, x_2} N_{x_1, x_2}^a \frac{d_{x_1} d_{x_2}}{\mathcal{D}^2} \log d_{x_2} \quad (\text{B9})$$

$$= d_a \sum_{x_1} \frac{d_{x_1}^2}{\mathcal{D}^2} \log d_{x_1} + d_a \sum_{x_2} \frac{d_{x_2}^2}{\mathcal{D}^2} \log d_{x_2} \quad (\text{B10})$$

$$= 2d_a \sum_x \frac{d_x^2 \log d_x}{\mathcal{D}^2}. \quad (\text{B11})$$

Assume Eq. (B8) holds for n -tuples, then

$$\sum_{\vec{x}_n, x_{n+1}} N_a(\vec{x}_{n+1}) \frac{\prod_{j \leq n+1} d_{x_j}}{\mathcal{D}^{2n}} \log \prod_{k \leq n+1} d_{x_k} = \sum_{\substack{\vec{x}_n \\ y_{n-1}, x_{n+1}}} N_{y_{n-1}}(\vec{x}_n) N_{y_{n-1}, x_{n+1}}^a \frac{\prod_{j \leq n} d_{x_j}}{\mathcal{D}^{2n}} d_{x_{n+1}} \log \left(\prod_{k \leq n} d_{x_k} d_{n+1} \right) \quad (\text{B12})$$

$$= \sum_{\substack{\vec{x}_n \\ y_{n-1}, x_{n+1}}} N_{y_{n-1}}(\vec{x}_n) \frac{\prod_{j \leq n} d_{x_j}}{\mathcal{D}^{2n}} N_{y_{n-1}, x_{n+1}}^a d_{x_{n+1}} \left(\log \prod_{k \leq n} d_{x_k} + \log d_{x_{n+1}} \right) \quad (B13)$$

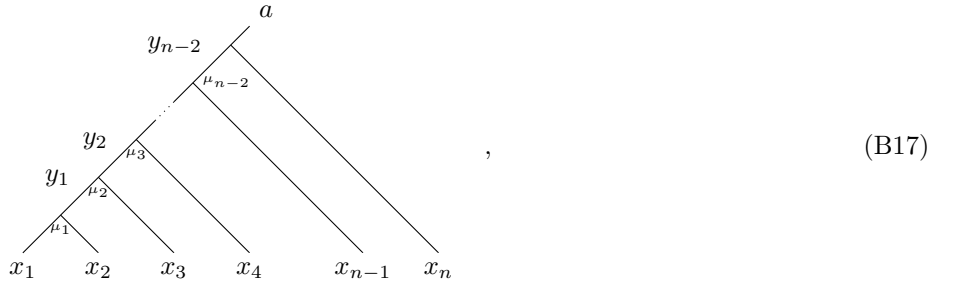
$$= n \sum_x \frac{d_x^2 \log d_x}{\mathcal{D}^2} \sum_{y_{n-1}, x_{n+1}} \frac{N_{y_{n-1}, x_{n+1}}^a d_{y_{n-1}} d_{x_{n+1}}}{\mathcal{D}^2} + \sum_{y_{n-1}, x_{n+1}} N_{y_{n-1}, x_{n+1}}^a \frac{d_{y_{n-1}} d_{x_{n+1}} \log d_{x_{n+1}}}{\mathcal{D}^2} \quad (B14)$$

$$= n d_a \sum_x \frac{d_x^2 \log d_x}{\mathcal{D}^2} \sum_{x_{n+1}} \frac{d_{x_{n+1}}^2 \log d_{x_{n+1}}}{\mathcal{D}^2} + d_a \sum_{x_{n+1}} \frac{d_{x_{n+1}}^2 \log d_{x_{n+1}}}{\mathcal{D}^2} \quad (B15)$$

$$= (n+1) d_a \sum_x \frac{d_x^2 \log d_x}{\mathcal{D}^2}. \quad (B16)$$

□

Lemma 6. Let \mathcal{C} a unitary fusion category. Given a fixed fusion outcome a on n simple objects, the probability of the tree



in the ground state of a topological loop-gas (Levin-Wen or Walker-Wang) model is

$$\Pr[\vec{x}, \vec{y}, \vec{\mu} | a] = \frac{\prod_{j \leq n} \Pr[x_j]}{\Pr[a] \prod_{k \leq n} d_{x_k}} d_a \quad (B18)$$

$$= \frac{\prod_{j \leq n} d_{x_j}}{d_a \mathcal{D}^{2(n-1)}}. \quad (B19)$$

Proof. Given a pair of objects a, b , the probability that they fuse to c is given by [28, 62]

$$\Pr[a \otimes b \rightarrow c] = \frac{N_{ab}^c d_c}{d_a d_b}, \quad (B20)$$

so the probability that $x_1 \otimes x_2 \otimes \dots \otimes x_n \rightarrow a$ is

$$\Pr[x_1 \otimes x_2 \otimes x_3 \otimes \dots \otimes x_n \rightarrow a] = \sum_{\vec{y}} \Pr[x_1 \otimes x_2 \rightarrow y_1] \Pr[y_1 \otimes x_3 \rightarrow y_2] \dots \Pr[y_{n-2} \otimes x_n \rightarrow a] \quad (B21)$$

$$= \frac{N_a(\vec{x})}{\prod_{j \leq n} d_{x_j}} d_a, \quad (B22)$$

where

$$N_a(\vec{x}) := \sum_{\vec{y}} N_{x_1 x_2}^{y_1} N_{y_1 x_3}^{y_2} \dots N_{y_{n-2} x_n}^a \quad (B23)$$

$$= \sum_{\vec{y}} N_a(\vec{x}, \vec{y}). \quad (B24)$$

The probability of a configuration is

$$\Pr[\vec{x}, \vec{y} | a] = \Pr[x_1 \otimes x_2 \otimes x_3 \otimes \dots \otimes x_n \rightarrow a] \frac{\prod_{j \leq n} \Pr[x_j]}{\Pr[a]} \quad (B25)$$

$$= \frac{N_a(\vec{x}, \vec{y}) d_a}{\prod_{k \leq n} d_{x_k}} \frac{\prod_{j \leq n} \Pr[x_j]}{\Pr[a]}, \quad (B26)$$

where $\Pr[x_i] = d_{x_i}^2 / \mathcal{D}^2$. For a fixed \vec{x} and \vec{y} , all (allowed) $\vec{\mu}$ are equally likely, and there are $N_a(\vec{x}, \vec{y})$ such configurations, so

$$\Pr[\vec{x}, \vec{y}, \vec{\mu} | a] = \frac{\prod_{j \leq n} \Pr[x_j]}{\Pr[a] \prod_{k \leq n} d_{x_k}} d_a \quad (B27)$$

$$= \frac{\prod_{j \leq n} d_{x_j}}{d_a \mathcal{D}^{2(n-1)}}. \quad (B28)$$

Lemma 4 can be used to show these are properly normalized. \square

Theorem 3. *For a Walker-Wang model defined by a unitary premodular category of one of the following types:*

1. $\mathcal{C} = \mathcal{A} \boxtimes \mathcal{B}$, where \mathcal{A} is symmetric and \mathcal{B} is modular [28],
2. \mathcal{C} pointed,
3. $\text{rk}(\mathcal{C}) < 6$ and multiplicity free,
4. $\text{rk}(\mathcal{C}) = \text{rk}(\mathcal{Z}_2(\mathcal{C})) + 1$ and $d_x = \mathcal{D}_{\mathcal{Z}_2(\mathcal{C})}$, where x is the additional object,

then Eq. (79) holds. As a consequence, the topological entanglement entropy (defined using the regions in Fig. 3) in the bulk is given by

$$\delta = \log \mathcal{D}_{\mathcal{Z}_2(\mathcal{C})}^2. \quad (B29)$$

As special cases, this includes

$$\delta_{\text{modular}} = 0 \quad (B30)$$

$$\delta_{\text{symmetric}} = \log \mathcal{D}^2 \quad (B31)$$

Proof.

1. Case 1

Using the premodular trap (Corollary 1), we have the matrix elements of $\mathcal{S}_c^\dagger \mathcal{S}_c$

$$[\mathcal{S}_c^\dagger \mathcal{S}_c]_{(a,\alpha),(b,\beta)} = \sqrt{\frac{d_c}{d_a d_b}} \sum_{x \in \mathcal{Z}_2(\mathcal{C}), \mu} \sqrt{d_x} \quad \text{Diagram: } \begin{array}{c} \text{A circle with labels } \alpha, \bar{a}, \mu, \bar{b}, \beta \text{ around the perimeter.} \\ \text{Inside the circle, there is a central point labeled } x. \\ \text{From } x, \text{ there are four lines:} \\ \text{1. Top-left line: } \alpha \text{ to } a. \\ \text{2. Top-right line: } \bar{a} \text{ to } \mu. \\ \text{3. Bottom-left line: } \mu \text{ to } \bar{b}. \\ \text{4. Bottom-right line: } \bar{b} \text{ to } \beta. \end{array} \quad (B32)$$

If \mathcal{C} is symmetric, $\mathcal{Z}_2(\mathcal{C}) = \mathcal{C}$, and

$$[\mathcal{S}_c^\dagger \mathcal{S}_c]_{(a,\alpha),(b,\beta)} = \delta_{c=1} d_a d_b. \quad (B33)$$

This matrix is rank 1, with eigenvalue \mathcal{D}^2 . If \mathcal{C} is modular, $\mathcal{Z}_2(\mathcal{C}) = \mathbf{Vec}$, and

$$[\mathcal{S}_c^\dagger \mathcal{S}_c]_{(a,\alpha),(b,\beta)} = \delta_{a=b} \delta_{\alpha=\beta} \delta_{\bar{a} \otimes a = c} d_c. \quad (B34)$$

For fixed c , this matrix is rank $\sum_c N_{\bar{a},a}^c$, with all eigenvalues equal to d_c .

If \mathcal{C} is pointed (every simple object has dimension 1), then $\mathcal{S}_c = 0$ unless $c = 1$. In this case, the fusion rules are given by a finite Abelian group A [33, 59], and $\mathcal{Z}_2(\mathcal{C}) = A'$ has fusion rules given by a subgroup. From Lemmas 1 and 2, along with symmetries of the \mathcal{S}_1 matrix proven in Ref. 34 we know that

$$[\mathcal{S}_1^\dagger \mathcal{S}_1]_{ab} = \sum_{c \in \mathcal{Z}_2(\mathcal{C})} N_{ab}^c d_c, \quad (\text{B35})$$

so

$$[\mathcal{S}_1^\dagger \mathcal{S}_1]_{ab} = 1 \iff a \in bA'. \quad (\text{B36})$$

Therefore, $[\mathcal{S}_1^\dagger \mathcal{S}_1]$ is a block matrix, with $[A : A'] = |A|/|A'|$ blocks, labeled by the cosets of A' , each full of ones. Therefore, there are $[A : A']$ eigenvalues, identically $\mathcal{D}_{\mathcal{Z}_2(\mathcal{C})}^2$. The entropy is given by

$$\delta = \log \mathcal{D}_{\mathcal{Z}_2(\mathcal{C})}^2. \quad (\text{B37})$$

3. Case 3

Case 3 is proven explicitly in the attached Mathematica file [38]. Classification of the fusion rings for ranks 2-5 can be found in Ref. 63–67, along with Ref. 68. Additionally, all multiplicity free fusion rings for ranks 1-6 can be found at Ref. 69. From this, explicit F and R data can be found. The list of categories, along with their properties, is included beginning Page 33.

4. Case 4

It is straightforward to check that if a or b are in $\mathcal{Z}_2(\mathcal{C})$, then

$$[\mathcal{S}_c^\dagger \mathcal{S}_c]_{(a,\alpha),(b,\beta)} = \delta_{c=1} d_a d_b \delta_{a \in \mathcal{Z}_2(\mathcal{C})} \delta_{b \in \mathcal{Z}_2(\mathcal{C})}, \quad (\text{B38})$$

so $\mathcal{S}_c^\dagger \mathcal{S}_c$ has the form

$$[\mathcal{S}_c^\dagger \mathcal{S}_c] = \mathcal{Z}_2(\mathcal{C}) \begin{bmatrix} d_a d_b \delta_{c=1} & 0 \\ 0 & X_c \end{bmatrix} = U \mathcal{Z}_2(\mathcal{C}) \begin{bmatrix} \mathcal{D}_{\mathcal{Z}_2(\mathcal{C})}^2 \delta_{c=1} & 0 & \cdots \\ 0 & 0 & \cdots & 0 \\ \vdots & \vdots & \ddots & \\ 0 & & & \tilde{X}_c \end{bmatrix} U^\dagger. \quad (\text{B39})$$

From the top left block, we have an eigenvector of $\mathcal{S}_1^\dagger \mathcal{S}_1$ with entries $v_a = \delta_{a \in \mathcal{Z}_2(\mathcal{C})} d_a$ with eigenvalue $\mathcal{D}_{\mathcal{Z}_2(\mathcal{C})}^2$. From Lemmas 1 and 2, along with symmetries of the \mathcal{S}_1 matrix proven in Ref. 34 we know that

$$[\mathcal{S}_1^\dagger \mathcal{S}_1]_{ab} = \sum_{c \in \mathcal{Z}_2(\mathcal{C})} N_{ab}^c d_c. \quad (\text{B40})$$

The vector with entries $w_a = d_a$ is also an eigenvector with the same eigenvalue:

$$\sum_{b \in \mathcal{C}} \sum_{c \in \mathcal{Z}_2(\mathcal{C})} N_{ab}^c d_c d_b = \sum_{c \in \mathcal{Z}_2(\mathcal{C})} d_a d_c^2 \quad (\text{B41})$$

$$= \mathcal{D}_{\mathcal{Z}_2(\mathcal{C})}^2 d_a, \quad (\text{B42})$$

so we have an orthogonal vector $w - v$ with eigenvalue $\mathcal{D}_{\mathcal{Z}_2(\mathcal{C})}^2$.

If $\text{rk}(\mathcal{C}) = \text{rk}(\mathcal{Z}_2(\mathcal{C})) + 1$ and the additional object has $d_x = \mathcal{D}_{\mathcal{Z}_2(\mathcal{C})}$, then all other eigenvalues must be 0 since

$$\delta = \log \mathcal{D}_{\mathcal{Z}_2(\mathcal{C})}^2. \quad (\text{B43})$$

□

5. Small category data

Data for small categories. “Valid” indicates that the pentagon, hexagon, and ribbon equations, along with unitarity, are true. “TY” indicates that the category has the property defined in Case 4 of Theorem 3.

Full data, including explicit F and R symbols is provided in the attached Mathematica files, also available at Ref. 38. Note that these may take *a very long time* to check. This is due to the complicated algebraic integers occurring, and Mathematica needing to simplify.

Categories are named $\text{FR}_{c;x}^{a,b}$ according to their fusion ring $\text{FR}_c^{a,b}$ from Ref. 69, along with their categorification ID x . Highlighted categories do not fall within any of the other cases in Theorem 3.

Cat. ID	Rank	\mathcal{D}^2	Valid	$\text{rk}(\mathcal{Z}_2(\mathcal{C}))$	Premodular?	Pointed?	TY?	TEE	$\log \mathcal{D}_{\mathcal{Z}_2(\mathcal{C})}^2$	Conjecture true?
$\text{FR}_{1;0}^{2,0}$	2	2	✓	2	Symm.	✓		$\log 2$	$\log 2$	✓
$\text{FR}_{1;1}^{2,0}$	2	2	✓	1	Mod.	✓	✓	0	0	✓
$\text{FR}_{1;2}^{2,0}$	2	2	✓	2	Symm.	✓		$\log 2$	$\log 2$	✓
$\text{FR}_{1;3}^{2,0}$	2	2	✓	1	Mod.	✓	✓	0	0	✓
$\text{FR}_{2;0}^{2,0}$	2	$\frac{1}{2}(\sqrt{5} + 5)$	✓	1	Mod.			0	0	✓
$\text{FR}_{2;1}^{2,0}$	2	$\frac{1}{2}(\sqrt{5} + 5)$	✓	1	Mod.			0	0	✓
$\text{FR}_{1;0}^{3,0}$	3	4	✓	1	Mod.			0	0	✓
$\text{FR}_{1;1}^{3,0}$	3	4	✓	1	Mod.			0	0	✓
$\text{FR}_{1;2}^{3,0}$	3	4	✓	1	Mod.			0	0	✓
$\text{FR}_{1;3}^{3,0}$	3	4	✓	1	Mod.			0	0	✓
$\text{FR}_{1;4}^{3,0}$	3	4	✓	1	Mod.			0	0	✓
$\text{FR}_{1;5}^{3,0}$	3	4	✓	1	Mod.			0	0	✓
$\text{FR}_{1;6}^{3,0}$	3	4	✓	1	Mod.			0	0	✓
$\text{FR}_{1;7}^{3,0}$	3	4	✓	1	Mod.			0	0	✓
$\text{FR}_{2;0}^{3,0}$	3	6	✓	3	Symm.			$\log 6$	$\log 6$	✓
$\text{FR}_{2;1}^{3,0}$	3	6	✓	2		✓		$\log 2$	$\log 2$	✓
$\text{FR}_{2;2}^{3,0}$	3	6	✓	2		✓		$\log 2$	$\log 2$	✓
$\text{FR}_{3;0}^{3,0}$	3	~ 9.30	✓	1	Mod.			0	0	✓
$\text{FR}_{3;1}^{3,0}$	3	~ 9.30	✓	1	Mod.			0	0	✓
$\text{FR}_{1;0}^{3,2}$	3	3	✓	3	Symm.	✓		$\log 3$	$\log 3$	✓
$\text{FR}_{1;1}^{3,2}$	3	3	✓	1	Mod.	✓		0	0	✓
$\text{FR}_{1;2}^{3,2}$	3	3	✓	1	Mod.	✓		0	0	✓

Cat. ID	Rank	\mathcal{D}^2	Valid	$\text{rk}(\mathcal{Z}_2(\mathcal{C}))$	Premodular?	Pointed?	TY?	TEE	$\log \mathcal{D}_{\mathcal{Z}_2(\mathcal{C})}^2$	Conjecture true?
FR _{1;0} ^{4,0}	4	4	✓	4	Symm.	✓		$\log 4$	$\log 4$	✓
FR _{1;1} ^{4,0}	4	4	✓	1	Mod.	✓		0	0	✓
FR _{1;2} ^{4,0}	4	4	✓	4	Symm.	✓		$\log 4$	$\log 4$	✓
FR _{1;3} ^{4,0}	4	4	✓	1	Mod.	✓		0	0	✓
FR _{1;4} ^{4,0}	4	4	✓	2	✓	✓		$\log 2$	$\log 2$	✓
FR _{1;5} ^{4,0}	4	4	✓	2	✓	✓		$\log 2$	$\log 2$	✓
FR _{1;6} ^{4,0}	4	4	✓	2	✓	✓		$\log 2$	$\log 2$	✓
FR _{1;7} ^{4,0}	4	4	✓	2	✓	✓		$\log 2$	$\log 2$	✓
FR _{1;8} ^{4,0}	4	4	✓	4	Symm.	✓		$\log 4$	$\log 4$	✓
FR _{1;9} ^{4,0}	4	4	✓	1	Mod.	✓		0	0	✓
FR _{1;10} ^{4,0}	4	4	✓	4	Symm.	✓		$\log 4$	$\log 4$	✓
FR _{1;11} ^{4,0}	4	4	✓	1	Mod.	✓		0	0	✓
FR _{1;12} ^{4,0}	4	4	✓	2	✓	✓		$\log 2$	$\log 2$	✓
FR _{1;13} ^{4,0}	4	4	✓	2	✓	✓		$\log 2$	$\log 2$	✓
FR _{1;14} ^{4,0}	4	4	✓	2	✓	✓		$\log 2$	$\log 2$	✓
FR _{1;15} ^{4,0}	4	4	✓	2	✓	✓		$\log 2$	$\log 2$	✓
FR _{1;16} ^{4,0}	4	4	✓	1	Mod.	✓		0	0	✓
FR _{1;17} ^{4,0}	4	4	✓	2	✓	✓		$\log 2$	$\log 2$	✓
FR _{1;18} ^{4,0}	4	4	✓	1	Mod.	✓		0	0	✓
FR _{1;19} ^{4,0}	4	4	✓	2	✓	✓		$\log 2$	$\log 2$	✓
FR _{1;20} ^{4,0}	4	4	✓	1	Mod.	✓		0	0	✓
FR _{1;21} ^{4,0}	4	4	✓	1	Mod.	✓		0	0	✓
FR _{1;22} ^{4,0}	4	4	✓	1	Mod.	✓		0	0	✓
FR _{1;23} ^{4,0}	4	4	✓	1	Mod.	✓		0	0	✓
FR _{1;24} ^{4,0}	4	4	✓	1	Mod.	✓		0	0	✓
FR _{1;25} ^{4,0}	4	4	✓	2	✓	✓		$\log 2$	$\log 2$	✓
FR _{1;26} ^{4,0}	4	4	✓	1	Mod.	✓		0	0	✓
FR _{1;27} ^{4,0}	4	4	✓	2	✓	✓		$\log 2$	$\log 2$	✓
FR _{1;28} ^{4,0}	4	4	✓	1	Mod.	✓		0	0	✓
FR _{1;29} ^{4,0}	4	4	✓	1	Mod.	✓		0	0	✓
FR _{1;30} ^{4,0}	4	4	✓	1	Mod.	✓		0	0	✓
FR _{1;31} ^{4,0}	4	4	✓	1	Mod.	✓		0	0	✓
FR _{2;0} ^{4,0}	4	$\sqrt{5} + 5$	✓	2	✓			$\log 2$	$\log 2$	✓
FR _{2;1} ^{4,0}	4	$\sqrt{5} + 5$	✓	1	Mod.			0	0	✓
FR _{2;2} ^{4,0}	4	$\sqrt{5} + 5$	✓	2	✓			$\log 2$	$\log 2$	✓
FR _{2;3} ^{4,0}	4	$\sqrt{5} + 5$	✓	1	Mod.			0	0	✓
FR _{2;4} ^{4,0}	4	$\sqrt{5} + 5$	✓	2	✓			$\log 2$	$\log 2$	✓
FR _{2;5} ^{4,0}	4	$\sqrt{5} + 5$	✓	1	Mod.			0	0	✓
FR _{2;6} ^{4,0}	4	$\sqrt{5} + 5$	✓	2	✓			$\log 2$	$\log 2$	✓
FR _{2;7} ^{4,0}	4	$\sqrt{5} + 5$	✓	1	Mod.			0	0	✓
FR _{3;0} ^{4,0}	4	10	✓	4	Symm.			$\log 10$	$\log 10$	✓
FR _{3;1} ^{4,0}	4	10	✓	2	✓			$\log 2$	$\log 2$	✓
FR _{3;2} ^{4,0}	4	10	✓	2	✓			$\log 2$	$\log 2$	✓
FR _{3;3} ^{4,0}	4	10	✓	2	✓			$\log 2$	$\log 2$	✓
FR _{3;4} ^{4,0}	4	10	✓	2	✓			$\log 2$	$\log 2$	✓
FR _{4;0} ^{4,0}	4	$4\sqrt{2} + 8$	✓	2	✓			$\log 2$	$\log 2$	✓
FR _{4;1} ^{4,0}	4	$4\sqrt{2} + 8$	✓	2	✓			$\log 2$	$\log 2$	✓
FR _{5;0} ^{4,0}	4	$\frac{1}{2}(5\sqrt{5} + 15)$	✓	1	Mod.			0	0	✓
FR _{5;1} ^{4,0}	4	$\frac{1}{2}(5\sqrt{5} + 15)$	✓	1	Mod.			0	0	✓
FR _{5;2} ^{4,0}	4	$\frac{1}{2}(5\sqrt{5} + 15)$	✓	1	Mod.			0	0	✓
FR _{5;3} ^{4,0}	4	$\frac{1}{2}(5\sqrt{5} + 15)$	✓	1	Mod.			0	0	✓
FR _{6;0} ^{4,0}	4	~ 19.24	✓	1	Mod.			0	0	✓
FR _{6;1} ^{4,0}	4	~ 19.24	✓	1	Mod.			0	0	✓
FR _{6;2} ^{4,0}	4	4	✓	4	Symm.	✓		$\log 4$	$\log 4$	✓
FR _{1;0} ^{4,2}	4	4	✓	1	Mod.	✓		0	0	✓
FR _{1;1} ^{4,2}	4	4	✓	2	✓	✓		$\log 2$	$\log 2$	✓
FR _{1;2} ^{4,2}	4	4	✓	1	Mod.	✓		0	0	✓
FR _{1;3} ^{4,2}	4	4	✓	2	✓	✓		0	0	✓
FR _{1;4} ^{4,2}	4	4	✓	4	Symm.	✓		$\log 4$	$\log 4$	✓
FR _{1;5} ^{4,2}	4	4	✓	1	Mod.	✓		0	0	✓
FR _{1;6} ^{4,2}	4	4	✓	2	✓	✓		$\log 2$	$\log 2$	✓
FR _{1;7} ^{4,2}	4	4	✓	1	Mod.	✓		0	0	✓

